TECHNICAL REPORT 1766
March 1998

Medium-Data-Rate HF Experimental Test Results

Using Modified Harris RF–3201E Transceiver and R–2368/URR Receiver

L. H. Pinck
T. A. Danielson
R. North

Space and Naval Warfare Systems Center
San Diego, CA 92152–5001

SPACE AND NAVAL WARFARE SYSTEMS CENTER
San Diego, California 92152–5001

H. A. Williams, CAPT, USN
Commanding Officer

R. C. Kolb
Executive Director

ADMINISTRATIVE INFORMATION

The work detailed in this report was performed for the Office of Naval Research by the Terrestrial Link Implementation Branch, Code D846, Space and Naval Warfare (SPAWAR) Systems Center, San Diego (SSC San Diego).

Released by
T. A. Danielson, Head
Terrestrial Link
Implementation Branch

Under authority of
D. O. Milstead, Head
Integrated Satellite and
Link Communications
Systems Division

SB

EXECUTIVE SUMMARY

OBJECTIVE

The objective of this project is to develop and test medium-data-rate (MDR), high-frequency (HF) groundwave point-to-point communication links. Modern communication demands create a tremendous need for additional bandwidth that this technology can help support. In coordination with current high-data-rate ultra-high-frequency (UHF) line-of-sight (LOS) link projects, MDR HF can provide the beyond-line-of-sight (BLOS) RF links to support implementation of higher capacity communication links and networking technologies. This will dramatically improve transport of data, greatly reduce dependence on "stove-pipe" communication systems, and improve carrier battle group (CVBG) and amphibious task group (ATG) operations efficiency.

This project developed and implemented a 64-kbps high-frequency (HF) beyond-line-of-sight (BLOS) communication link within a 50-kHz, 3-dB bandwidth frequency channel. This is one of several efforts that attempts to increase the data rates that are commonly used in the HF band within the Navy for intra-ship BLOS communications. This project is funded by Drs. Rabinder Madan, Sherman Gee, and Neil Gerr of the Office of Naval Research (ONR).

METHOD

The MDR HF system is based on commercial products as well as existing radio equipment with simple modifications. The tests performed included laboratory and over-the-air operational tests. The laboratory portion included baseline characterization, static multipath, and dynamic multipath performance tests performed at Space and Naval Warfare System Center, San Diego (SSC San Diego) primarily between March and June 1997. The over-the-air tests were conducted over the 65-nmi seawater path between Wilson Cove at San Clemente Island (SCI), California, and SSC San Diego Building 40 on Point Loma, California, in September 1997. Many variations of different parameters including modulation, coding, and frequency were tested for both the laboratory and over-the-air tests to increase its bandwidth efficiency and thus increase its operational data rates within the 50-kHz bandwidth.

CONCLUSIONS

This report describes many MDR HF BLOS communication experiments and tests to prove the feasibility of using higher data rate in the HF frequency band. It was confirmed that the HF surface-wave channel over seawater is basically a benign channel that is primarily degraded by distance, frequency, and interferers. Many modulation and coding combinations were tested and quadrature phse-shift keying (QPSK) Viterbi ¾ and ½ clearly outperformed the other combinations in the laboratory as well as in the operational tests.

The operational tests between SCI and SSC San Diego were successful, so the next logical and needed step is an operational experiment between two deployed Navy ships during a Navy Exercise. This will be accomplished between USS *Coronado,* AGF 11, and USS *Cleveland,* LPD 7, during RIMPAC-98 in July and August 1998. The goal is to continue to prove the feasibility of the successful use of higher data rate HF links within the U.S. Navy, with proper modulation, coding, and frequencies for improved intership BLOS communications.

CONTENTS

Figures

Figures (Continued)

Tables

1. INTRODUCTION

This report describes the experimental test results of a medium-data-rate[1] (MDR), high-frequency (HF) groundwave point-to-point, full-duplex data link. This system uses relatively simple modifications of existing radio equipment and a commercial programmable satellite communications (SATCOM) modem. The goal is to develop and implement a 128-kbps Beyond-Line-Of-Sight (BLOS) HF communication link within a 50-kHz, 3-dB bandwidth frequency channel. This is one of several efforts that attempts to increase the data rates that are commonly used in the HF band within the Navy for intra-ship BLOS communications. Drs. Rabinder Madan, Sherman Gee, and Neil Gerr of the Office of Naval Research (ONR) funded this project.

The tests performed included laboratory back-to-back and over-the-air operational tests. The laboratory portion of these tests was performed at Space and Naval Warfare (SPAWAR) Systems Center, San Diego (SSC San Diego), primarily between March and June of 1997. In September 1997, the over-the-air tests were conducted over the 65-nmi seawater path between Wilson Cove at San Clemente Island (SCI), California, and Building 40, SSC San Diego, on Point Loma, California.

1.1 BACKGROUND

For many years, the Navy has used the HF portion (2 to 30 MHz) of the radio spectrum for voice and low-data-rate communications at ranges from line-of-sight (LOS) to thousands of miles. The U.S. Navy has discontinued regular use of HF for long-range communications (>500 nmi), but uses it intensively for intraship tactical communications, providing BLOS coverage up to several hundred miles. At these ranges, the surface wave mode of propagation (vice the skywave refractive mode) can provide good communications performance around the clock with proper frequency and antenna selection. Since the HF surface wave does not typically have the multiple path and fading problems associated with HF skywave refraction, it is said to be "non-dispersive" and regularly provides a higher quality channel (Sailors, 1997). It can potentially support channels of much greater bandwidth than those normally used for HF skywave communications. Current HF communications channels use a bandwidth of 3 kHz or less and are assigned and used for voice and data. Current modem technology supports maximum data rates of 4.8 kbps (2.4 kbps typical) and uses a standardized modem waveform such as the single-tone serial waveform of MIL–STD–188–110A.

The potential for increased data rates over HF comes at a time when information technology initiatives (Information Technology for the 21st Century (IT-21), Joint Maritime Communication Systems (JMCOMS), Advanced Digital Network System (ADNS), etc.) are creating a tremendous need for additional bandwidth for both intraship and ship-to-shore connectivity. While intraship data rates approaching T1 (1.544 Mbps) have been demonstrated over UHF LOS links (North et al. 1995), BLOS data links remain limited to 2.4 kbps over limited SATCOM and HF channels. Ship-to-shore links are similarly limited except for major combatants with super high-frequency (SHF) satellite systems.

---

[1] In this text, a low data rate (LDR) refers to any data rate less than 64 kilobits per second (kbps), a medium data rate (MDR) refers to any data rate between 64 kbps and 1536 kbps, and a high data rate (HDR) is equal to or greater than 1536 kbps.

The feasibility of higher HF data rates was demonstrated in an earlier developmental effort sponsored by Naval Coastal System Station (Panama City, FL) to develop a BLOS telemetry link between an autonomous semi-submersible mine hunter and its parent vessel. This experiment was successfully conducted using data rates of 56 kbps and 75 kbps over the 65-nmi seawater path between Wilson Cove at SCI and SSC San Diego, Building 40. This experiment used a programmable SATCOM modem operating a quadrature phase-shift keying (QPSK) waveform using a concatenated forward-error-correction coding technique (Reed-Solomon outer block code and a rate ¾ convolutional inner code). Transmit power was a nominal 10 watts from a matched whip antenna, and the information bandwidth was 40 kHz. While this link performed well over long periods (several hours), outages and periods of poor bit-error-rate (BER) performance were frequent. The exact cause of these outages is not known, but is presumed to be due to a combination of interference from nearby HF users and noise from man-made and natural sources. Nevertheless, the limited positive results of these 1995 tests laid the groundwork for the present effort sponsored by the Office of Naval Research, with the goal of improving the reliability and bandwidth efficiency of these links.

This report describes an improved implementation of this equipment based on a modified Harris RF-3021E Hawk transceiver and a modified R-2368R/URR receiver.

2. LABORATORY TESTS

2.1 EQUIPMENT DESCRIPTION AND SYSTEM SETUP

The equipment used in these tests consist of a commercial off-the-shelf (COTS) ComStream CM701 SATCOM modem, a modified nondevelopmental item (NDI) Harris RF-3021E Hawk transceiver, a modified NDI Harris R-2368/URR receiver, and other laboratory equipment, as needed. The Harris transceiver and receiver were both modified to provide a 40-kHz bandwidth and a 70.455-kHz intermediate frequency (IF) input or output, respectively. Noise-loaded measurements revealed that the transceiver has a 3-dB bandwidth of 60 kHz and that the receiver has the system band-limiting, 3-dB bandwidth of 50 kHz. Other modems, including those optimized for LOS and/or BLOS operation, will be tested when they become available in the near future.

The laboratory tests consisted of two sets: baseline performance and multipath performance. The first set of tests determines equipment baseline performance and is described in section 2.2. The second set of tests determines equipment static and dynamic multipath propagation performance and is described in sections 2.3 and 2.4, respectively. Figures 1 and 2, respectively, show the equipment test setup for the laboratory baseline and multipath tests. Both test setups used the Telecommunications Techniques Corporation (TTC) Fireberd 6000A bit-error tester to generate data and to detect and report BER statistics. The baseline tests setup used the Noise/Comm UFX-BER-8 to accurately set the signal-to-noise levels at the receiver. The multipath tests setup used the Telecom Analysis Systems, Inc TAS 4500 Multipath Emulator to add both static and dynamic multipaths in a controlled and repeatable fashion.

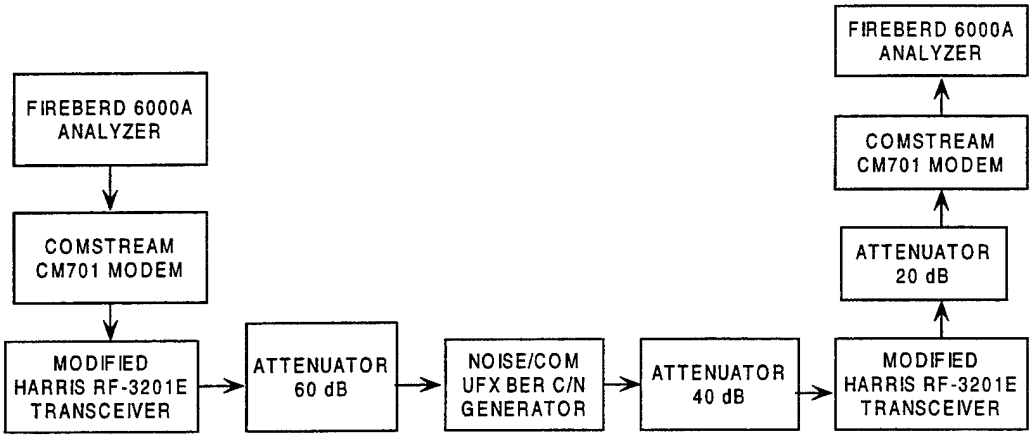

Figure 1. Equipment setup for baseline performance.

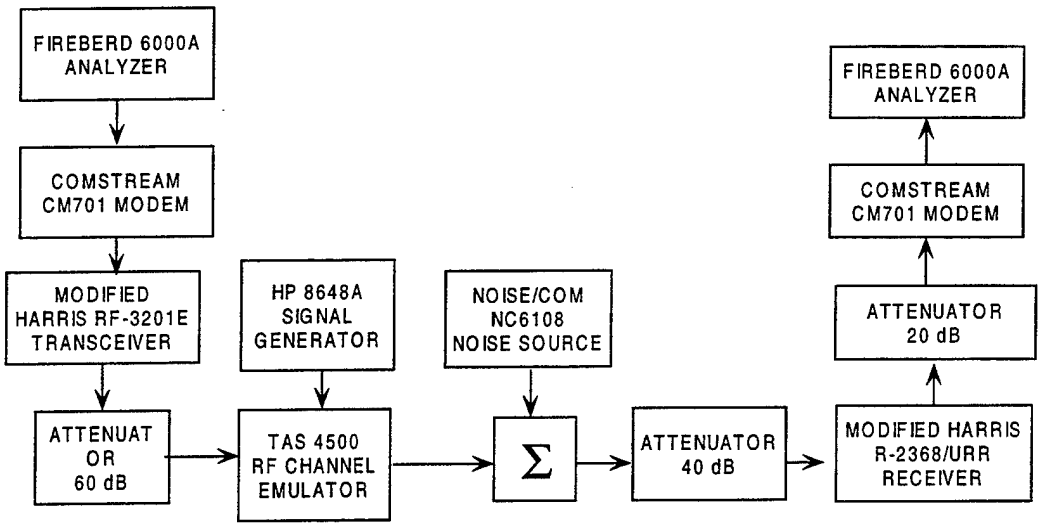

Figure 2. Equipment setup for multipath simulation test.

The object of these experimental tests was to determine the best configuration of the CM701 modems to support the highest and most reliable data rate. Table 1 lists modem configurations, data rates, 3-dB transmit bandwidths, symbol rates, and symbol durations that were tested. The modulation used was either uncoded binary phase-shift keying (BPSK) or coded QPSK. The forward-error-correction codes tested were convolutional, and concatenated Reed-Solomon (R-S) outer code with a convolutional inner code. The convolutional codes are decoded using a Viterbi decoding algorithm tested with a code rate of ½ and ¾. The symbol rate, Rs, is the data rate divided by number of bits per symbol times coding rate and is approximately equal to the 3-dB bandwidth (in hertz) of the transmitted signal. The symbol duration, Ts, is the inverse of the symbol rate. The bandwidth efficiency of a code is defined as the ratio of the information data rate to the 3-dB bandwidth. BPSK Uncoded and QPSK Viterbi rate ½ have a bandwidth efficiency of 1 bps/Hz, QPSK Viterbi rate ¾ has a bandwidth efficiency of 1.5 bps/Hz, and the QPSK concatenated coding scheme (Reed-Solomon rate 239/256 and Viterbi rate ¾) have a bandwidth efficiency of 1.4 bps/Hz. It should be noted that this system is capable of any data rate (in 1 bps increments) from 4.8 kbps up to 2.34 Mbps. The data rate of 20.8 kbps was chosen for comparison with the SICOM VIPER HF modem.

Table 1. CM701 configuration modes and data rates used in this report.

Modulation and Coding	Bandwidth Efficiency (bps/Hz)	Data Rate (kbps)	3 dB TX BW (kHz)	Symbol Rate (ksps)	Symbol Duration (μsec)
BPSK, Uncoded	1.0	20.8	20.8	20.8	48.08
		56.0	56.0	56.0	17.86
		70.0	70.0	70.0	14.29
QPSK, Viterbi ½	1.0	20.8	20.8	20.8	48.08
		56.0	56.0	56.0	17.86
		70.0	70.0	70.0	14.29
QPSK, R-S/ Viterbi ¾	1.4	20.8	14.85	14.85	67.32
		56.0	39.99	39.99	25.01
		70.0	49.99	49.99	20.00
QPSK, Viterbi ¾	1.5	20.8	13.87	13.87	72.12
		56.0	37.33	37.33	26.79
		70.0	46.67	46.67	21.43

2.2 BASELINE TEST RESULTS

2.2.1 Received Signal Level Performance

The first set of tests included characterizing the baseline equipment setup by conducting a back-to-back, transceiver-to-receiver test. Figure 3 shows the baseline characterization for BPSK Uncoded, QPSK Viterbi ½, and QPSK Viterbi ¾ for 56 kbps and QPSK Viterbi ½ for 20.8 kbps, where the averaged BER is plotted against the received signal level. Figure 3 highlights two separate performance issues. The first issue is due to the forward-error-correction coding and results in an improvement in the required receiver power needed to obtain a given BER. The second issue is due to inter-symbol interference (ISI) created by band-limiting in the R-2368/URR receiver that results in decreased performance. The next section describes these two issues in more detail. Figure 3 shows excellent receiver sensitivity for transmit bandwidths less than about 56 kHz.

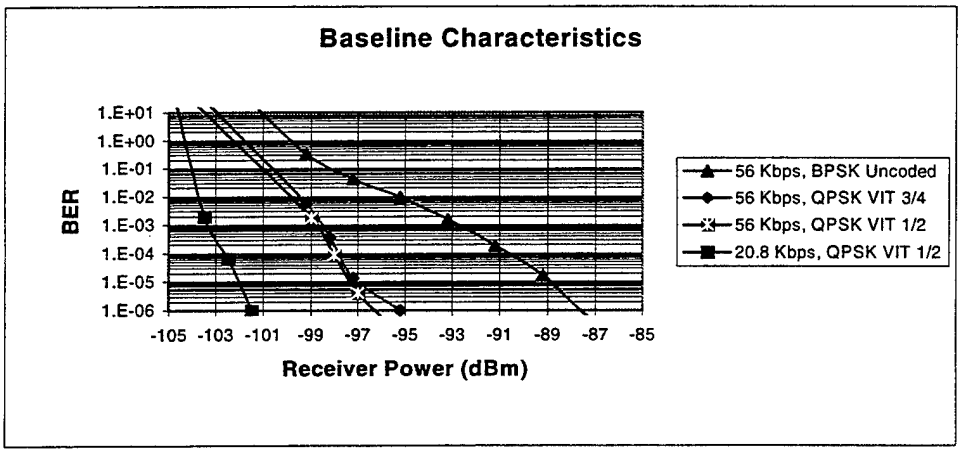

Figure 3. BER versus receiver power for baseline back-to-back characteristics.

2.2.2 E_b/N_o Performance

The next baseline tests were measured using a Noise/Com UFX BER C/N generator to add noise and calculate E_b/N_o (E_b= signal energy in one information bit, N_o= noise power per hertz) and the TTC Fireberd 6000A to perform BER measurements. These measurements assume an ideal channel with no interference or multipath effects. The results are shown in BER versus E_b/N_o graphs for QPSK Viterbi ½, QPSK Viterbi ¾, and BPSK Uncoded.

Each graph in figures 4 through 6 shows three modulation types and the theoretical BPSK curve for the data rates of 20.8 kbps, 56 kbps, and 70 kbps. Table 2 shows the results for the loss/gain for the various modulations summarized for a BER equal to $1x10^{-6}$. The implementation loss is measured between the theoretical BPSK curve and the measured BPSK Uncoded data. As the symbol rate increases beyond 50 ksps, the signal is degraded due to ISI caused by the system limiting the receiver bandwidth to about 50 kHz (Yacoub, 1993). This is apparent in figure 5 at 56 kbps (56 ksps), where the total loss for BPSK Uncoded increases over that in figure 4 at 20.8 kbps (20.8 ksps) because of the addition of the ISI loss. This BPSK Uncoded loss in figure 5 consists of the 1.2-dB implementation loss (from figure 4) plus over 7-dB ISI loss at BER=$1x10^{-6}$. As seen in figure 6, at 70 kbps (70 ksps), the total degradation is much larger and not measurable from our data at BERs larger than $1x10^{-3}$.

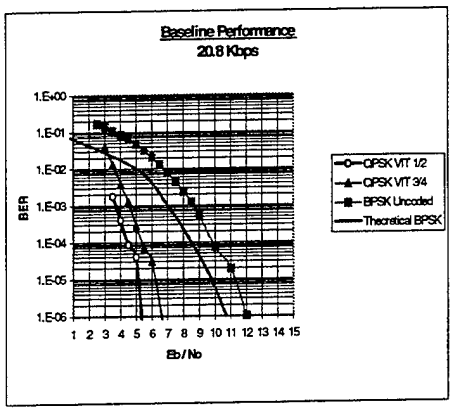

Figure 4. Data rate of 20.8 kbps.

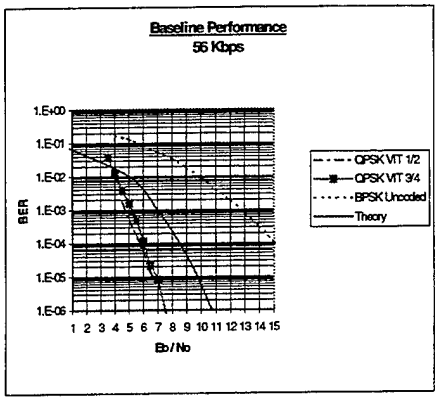

Figure 5. Data rate of 56 kbps.

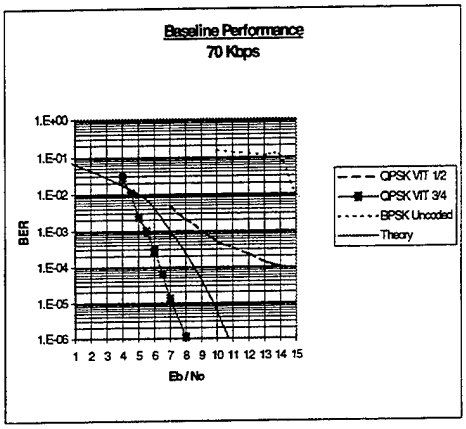

Figure 6. Data rate of 70 kbps.

The coding gain is measured by comparing the coded modulation data with the theoretical BPSK Uncoded data. As shown in figure 4 at 20.8 kbps, the coding gain for QPSK Viterbi ½ (20.8 ksps) is larger than for QPSK Viterbi ¾ (13.87 ksps). The coding gain is larger because there is more coding redundancy added in rate ½ than rate ¾. In figure 5, at 56 kbps, the coding gain for QPSK Viterbi ½ (56 ksps) is band-limited slightly, which results in a few decibels (2.2 dB) degradation due to ISI. However, QPSK Viterbi ¾ at 56 kbps (37.3ksps) is not band-limited and, thus, results in coding gain similar to that at 20.8 kbps. In figure 6, at 70 kbps, both BPSK Uncoded and QPSK Viterbi ½ (70 ksps) are so degraded from ISI that neither modulation is usable. QPSK Viterbi ¾ (46.7 ksps) results in only a slight degradation due to ISI and is the only usable modulation at 70 kbps.

The baseline performance results show that as long as the transmitted symbol rate is 56 ksps or less and that at least some forward-error-correction coding is applied, the modified HF equipment and CM701 modem can be expected to provide reasonable performance on an Additive White Gaussian Noise (AWGN) channel. The following sections investigate the performance of the equipment to static multipath (section 2.3) and to a dynamic multipath-fading (section 2.4) environment.

Table 2. Uncoded BPSK total loss and coding gain at 1 x 10^{-6} BER.

Data Rate (kbps)	Total Loss (dB) Implementation + ISI Loss	Coding Gain (dB)	
		Viterbi ½	Viterbi ¾
20.8	1.2	5.5	4.0
56	> 9	3.3	3.3
70	> 10	> -20	2.8

2.3 STATIC MULTIPATH TEST RESULTS

Since the CM701 modem was designed for SATCOM application, it does not incorporate any multipath compensation techniques. The multipath tests in this section and the following section were conducted to determine just how robust the simple waveforms (BPSK and QPSK) are when combined with various types of forward-error-correction codes. These results will be used to compare against other modem designs that do compensate for multipath.

The static (and dynamic) multipath test results were measured using the TAS 4500 RF Channel Emulator to add multiple propagation paths with various delays and losses. The tests in this section show the performance of the system to static multipath (e.g., fixed phase, amplitude, and delay). The static multipath tests were performed at 56 kbps and included an equal strength second path, a –3-dB loss second path, and a –10-dB loss second path, all at various differential delays.

2.3.1 Equal-Strengh Multipath

Figure 7 shows the test results for two equal-strength propagation paths with a differential delay of 15 µsec. A 15-µsec differential delay translates to a differential distance of about 4500 meters (2.4 nmi). Referring to table 1 for 56 kbps, note that the symbol duration for BPSK Uncoded and QPSK Viterbi ½ is 17.9 µsec and that the symbol duration for QPSK Viterbi ¾ is 26.8 µsec. Thus, the differential delay of 15 µsec is a significant portion of the symbol duration (84 percent and 56 percent, respectively). As a result, the figure illustrates significant degradation in performance for BPSK Uncoded and QPSK Viterbi ½. The maximum delay without loosing BER synchronization was 18 µsec for BPSK Uncoded, 17 µsec for QPSK Viterbi ½, and 26 µsec for QPSK Viterbi ¾, relating to approximately the symbol duration for the respective modulation.

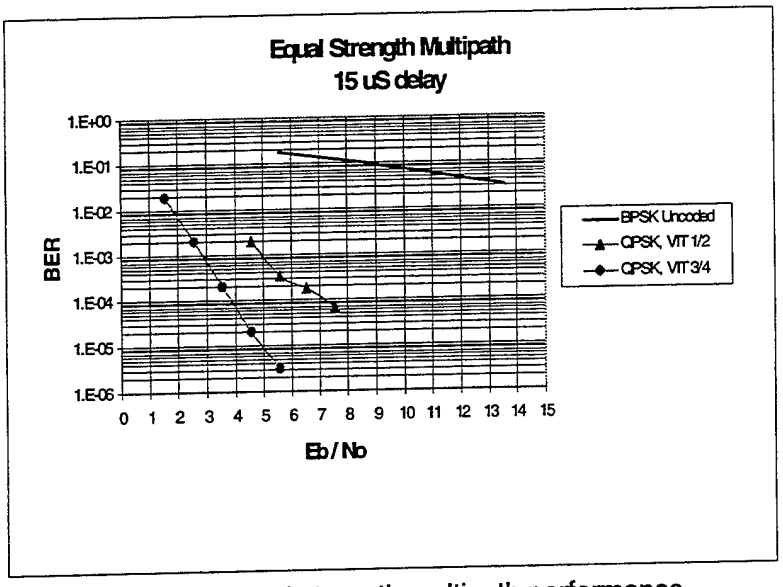

Figure 7. Equal-strength multipath performance.

2.3.2 –3-dB Multipath

Figures 8 and 9 are both plots of QPSK Viterbi ¾ at 56 kbps for two propagation paths. The signal strength of the second path is 3 dB below that of the main path. Figure 8 plots the BER versus E_b/N_o results for differential propagation delays of 5 µsec, 10 µsec, and 20 µsec. Figure 9 plots the E_b/N_o required for the system to maintain an average BER of 1×10^{-3} as a function of propagation delay of the second path. Generally, the system begins to degrade when the differential propagation delay is equal to approximately 10 percent of the symbol duration with complete failure occurring at between 80 to 100 percent of the symbol duration. The longest delay for QPSK Viterbi ¾ at 56 kbps to remain in synchronization was 20 µsec while the symbol duration is 26.8 µsec (symbol rate of 37.3 ksps).

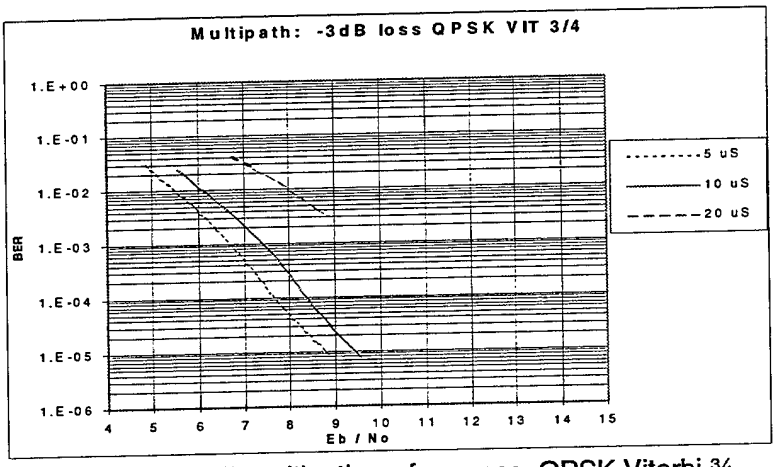

Figure 8. –3-dB multipath performance, QPSK Viterbi ¾.

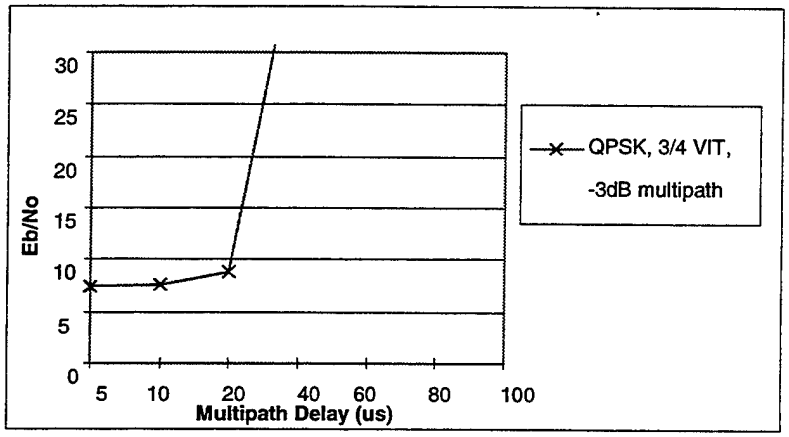

Figure 9. E_b/N_o versus multipath delay at 10 to 3 BER for –3-dB multipath.

2.3.3 –10-dB Multipath

Additional tests are presented in figures 10 through 12 for BPSK Uncoded, QPSK Viterbi ½, and QPSK Viterbi ¾, respectively, with the signal strength of the multipath 10 dB below the main path. During these tests, the TTC Fireberd 6000A remained synchronized for all the tested delays ranging from 5 to 100 µsec. The results show that QPSK VIT ½ performs better than either BPSK Uncoded or QPSK Viterbi ¾.

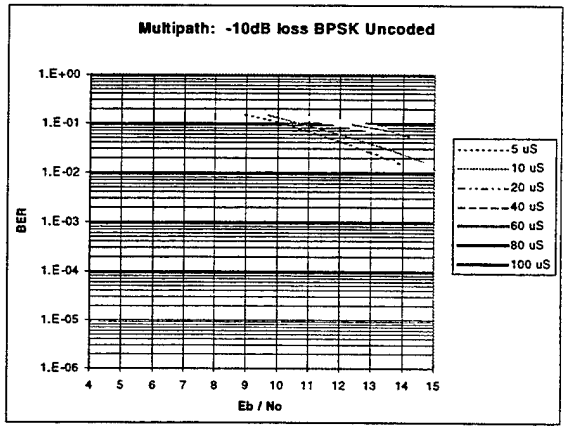

Figure 10. –10-dB multipath, BPSK Uncoded.

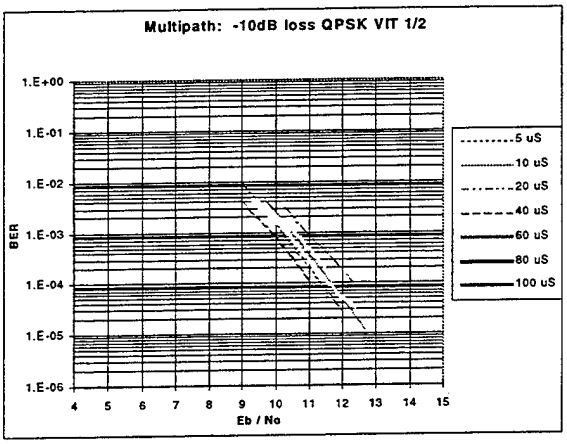

Figure 11. –10-dB multipath Viterbi ½.

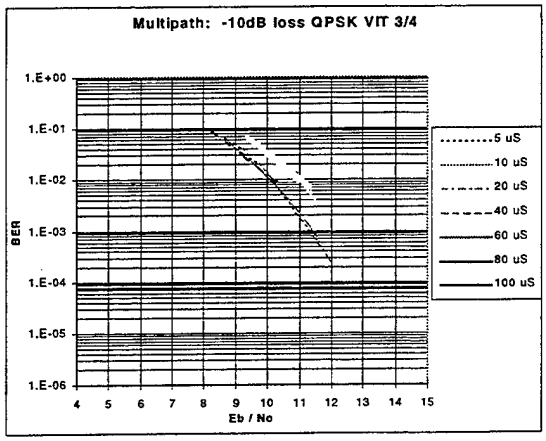

Figure 12. –10-dB multipath Viterbi ¾.

2.3.4 "M-Plot" Results

A standard multipath test used for characterization of the receiver multipath performance is called an "M Plot." The M Plot is created by using a two-path environment where the multipath signal with differential delay equal to 10 percent of the symbol duration creates a single, deep notch in the spectrum of the received signal. Adjusting the phase of the multipath varies the notch frequency, while adjusting the magnitude of the multipath varies the depth of the notch. The notch frequency is stepped through the spectrum of the received signal while the notch depth is varied until the BER is reduced to 1 x 10^{-6}. Figure 13 plots the resulting notch characteristics for BPSK Uncoded, QPSK Viterbi ½, and QPSK Viterbi ¾, where the carrier frequency is at 25 MHz. This figure indicates that QPSK Viterbi ½ and QPSK Viterbi ¾ are both more robust to multipath than BPSK Uncoded when the resulting notch is centered +/–5 kHz of the carrier frequency. Overall, QPSK Viterbi ¾ appears to provide the best overall performance with respect to multipath due to its robust waveform and reduced transmitted bandwidth (or equivalently, its longer symbol duration).

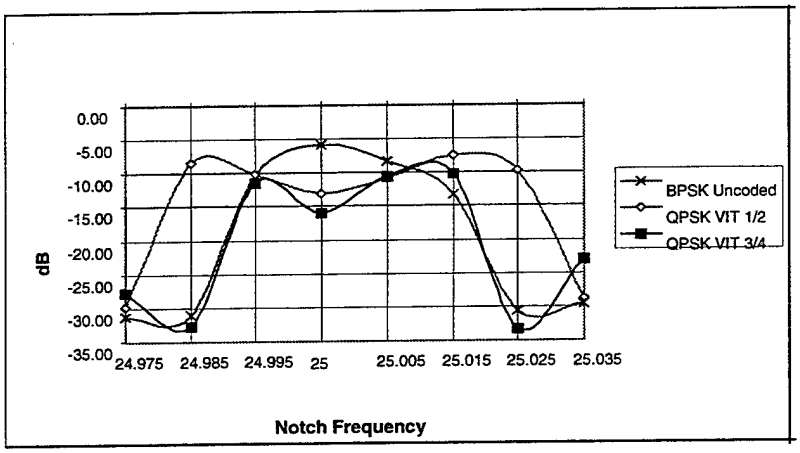

Figure 13. "M Plot" (notch depth versus notch frequency) for 56 kbps.

2.4 DYNAMIC MULTIPATH FADING RESULTS

The dynamic multipath channels are based on the three standard UHF LOS channels used by the HDR LOS program including the ship-to-ship, ship-to-shore, and ship-to-air channels. While the three test channels are discussed in this section, it is realized that these channels are only appropriate for UHF LOS communications. Nevertheless, the results will be useful when comparing CM701-based system performance with the performance of other modems. Three additional dynamic multipath channels are also tested based on 1-Hz fading variations of the three standard UHF LOS channels used specifically for HF communications.

The objective of these tests is to compare each of the four modulation types when used in dynamic multipath channels. The key measurements include the error analysis seconds (EAS), which are the seconds that the system remains in synchronization, and the error-free error-analysis seconds (EF EAS), which are those EAS that are error-free. The following data were collected for over 15 minutes and report the total EAS and EF EAS for each minute. The modeled channels get progressively more difficult from slow to fast channels as well as from ship-to-ship, ship-to-shore, and ship-to-air channels. As expected, the QPSK convolutional coded results improve upon the BPSK Uncoded results. The concatenated coded results perform worst because the system could not maintain the synchronization required by the additional block coding.

2.4.1 "Ship-to-Ship" Model

The first channels to model were a slow and a standard UHF LOS ship-to-ship fading channel. The slow channel is modeled as described in the following paragraphs:

2.4.1.1 Slow Ship-to-Ship Model. The slow channel is modeled as:

Path #1: GSM Rician, $F_d = 1$ Hz

Path #2: Rayleigh, $T_{1\text{-}2} = 0.01$ µsec, $F_d = 1$ Hz, $L_{1\text{-}2} = -6$ dB

The GSM Rician and Rayleigh models are included in the TAS 4500 software for the fading statistics of the envelope of the multipath signal.

Figure 14 shows the 15-minute slow ship-to-ship channel test results for BPSK Uncoded, QPSK Viterbi ½, QPSK Viterbi ¾, and QPSK R-S/Viterbi ¾. The first three modulations performed well with almost all the EAS at 60 seconds (most possible in 1 minute) and EF EAS above 50 seconds. Both QPSK-coded options added an average improvement of 1 to 2 seconds each minute over BPSK Uncoded. The QPSK R-S/Viterbi ¾ concatenated coding modulation technique did not perform well due to the long times required to resynchronize the CM701 demodulator after a fading-induced outage occurred.

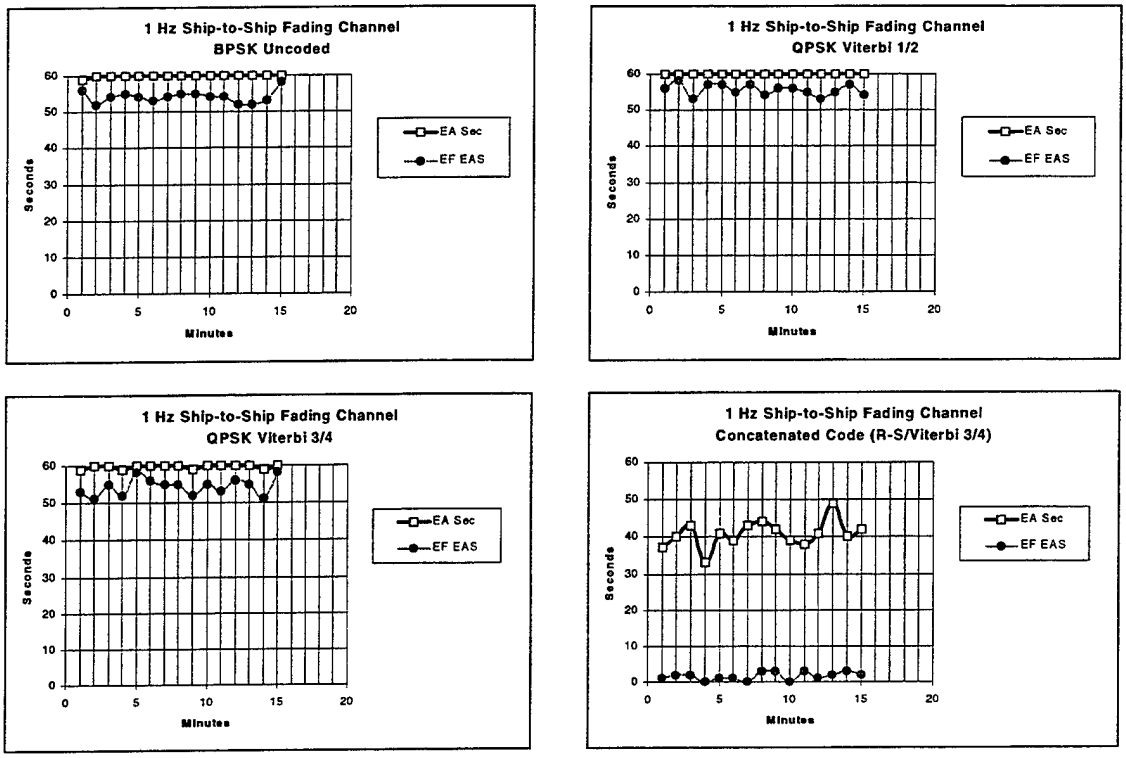

Figure 14. Slow ship-to-ship channel results (fade rate = 1 Hz).

2.4.1.2 Standard Ship-to-Ship Model. The standard UHF LOS ship-to-ship fading channel is modeled as:

Path #1: GSM Rician, $F_d = 1$ Hz

Path #2: Rayleigh, $T_{1\text{-}2} = 0.01$ μsec, $F_d = 10$ Hz, $L_{1\text{-}2} = -6$ dB

Figure 15 shows the 15-minute standard ship-to-ship channel test results for BPSK Uncoded, QPSK Viterbi ½, QPSK Viterbi ¾, and QPSK R-S/Viterbi ¾. The system performance degrades in the faster fading ship-to-ship channel due to the more rapid fading conditions. Interestingly, BPSK Uncoded, QPSK Viterbi ½, and QPSK Viterbi ¾ still had almost all the EAS at 59 to 60 seconds but the EF EAS decreased to only around 30 seconds.

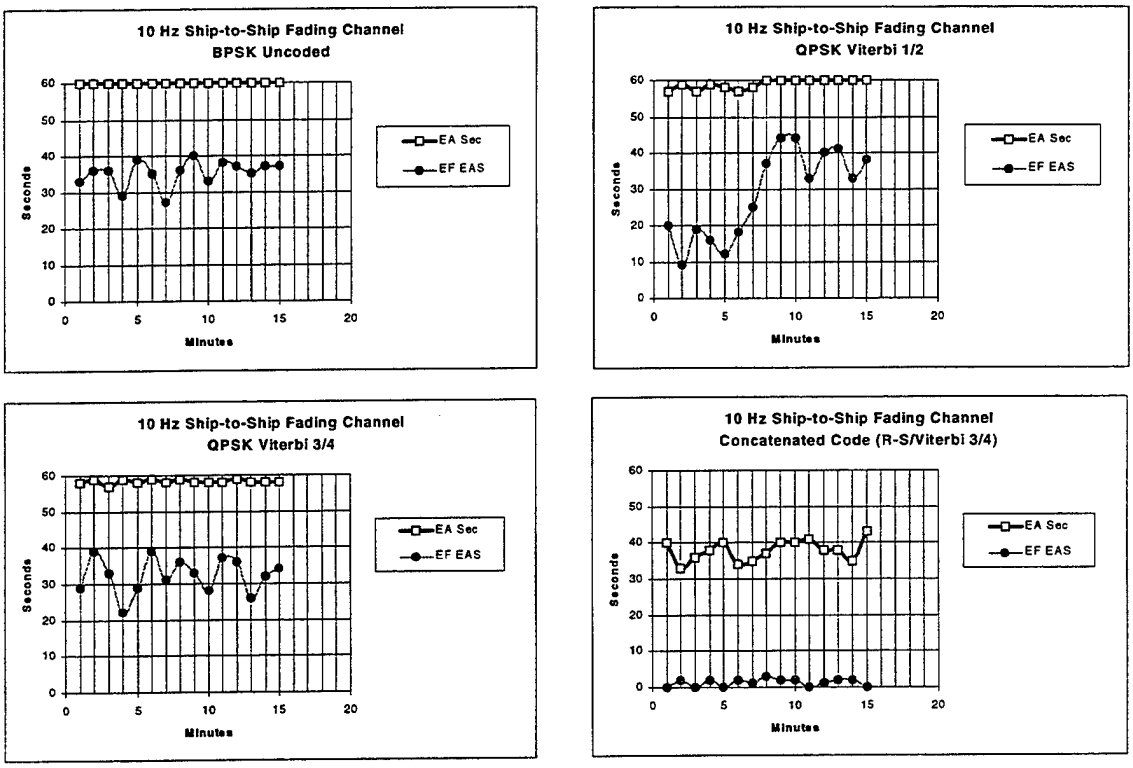

Figure 15. Standard ship-to-ship channel results (fade rate = 10 Hz).

2.4.2 "Ship-to-Shore" Model

The next channels to model were a slow and a standard UHF LOS ship-to-shore fading channel.

2.4.2.1 Slow Ship-to-Shore Model. The slow channel is modeled as:

Path #1: GSM Rician, $F_d = 1$ Hz

Path #2: Rayleigh, $T_{1-2} = 0.07$ μsec, $F_d = 1$ Hz, $L_{1-2} = -5$ dB

Path #3: Rayleigh, $T_{1-3} = 0.80$ μsec, $F_d = 1$ Hz, $L_{1-3} = -15$ dB

This model has a third propagation path along with longer differential delays than the ship-to-ship channels. Note that the differential delays are still significantly less than the symbol durations. Thus, the ship-to-shore channel behaves like a flat, fading channel, as did the ship-to-ship channel.

Figure 16 shows the ship-to-shore channel results for BPSK Uncoded, QPSK Viterbi ½, QPSK Viterbi ¾, and QPSK R-S/Viterbi ¾. Both QPSK-coded modulations outperform BPSK Uncoded by an average of 10 EF EAS seconds each minute. Again, the QPSK R-S/Viterbi ¾ modulation schemes did not perform well due to long resynchronization times.

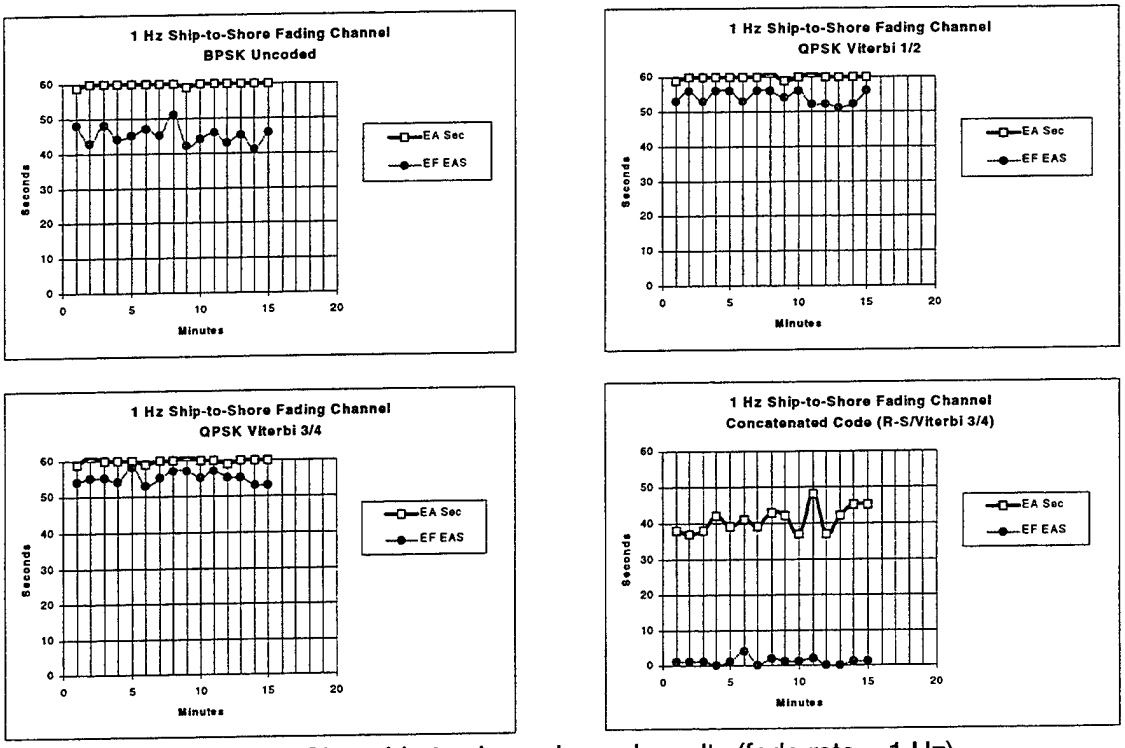

Figure 16. Slow ship-to-shore channel results (fade rate = 1 Hz).

2.4.2.2 Standard Ship-to-Shore Model. The standard UHF LOS ship-to-shore fading channel is modeled as:

Path #1: GSM Rician, $F_d = 10$ Hz

Path #2: Rayleigh, $T_{1-2} = 0.07$ µsec, $F_d = 10$ Hz, $L_{1-2} = -5$ dB

Path #3: Rayleigh, $T_{1-3} = 0.80$ µsec, $F_d = 10$ Hz, $L_{1-3} = -15$ dB

Figure 17 shows the standard ship-to-shore channel results for BPSK Uncoded, QPSK Viterbi ½, QPSK Viterbi ¾, and QPSK R-S/Viterbi ¾. These results are degraded from the previous slow version of this channel with an average EF EAS of 15 seconds or less.

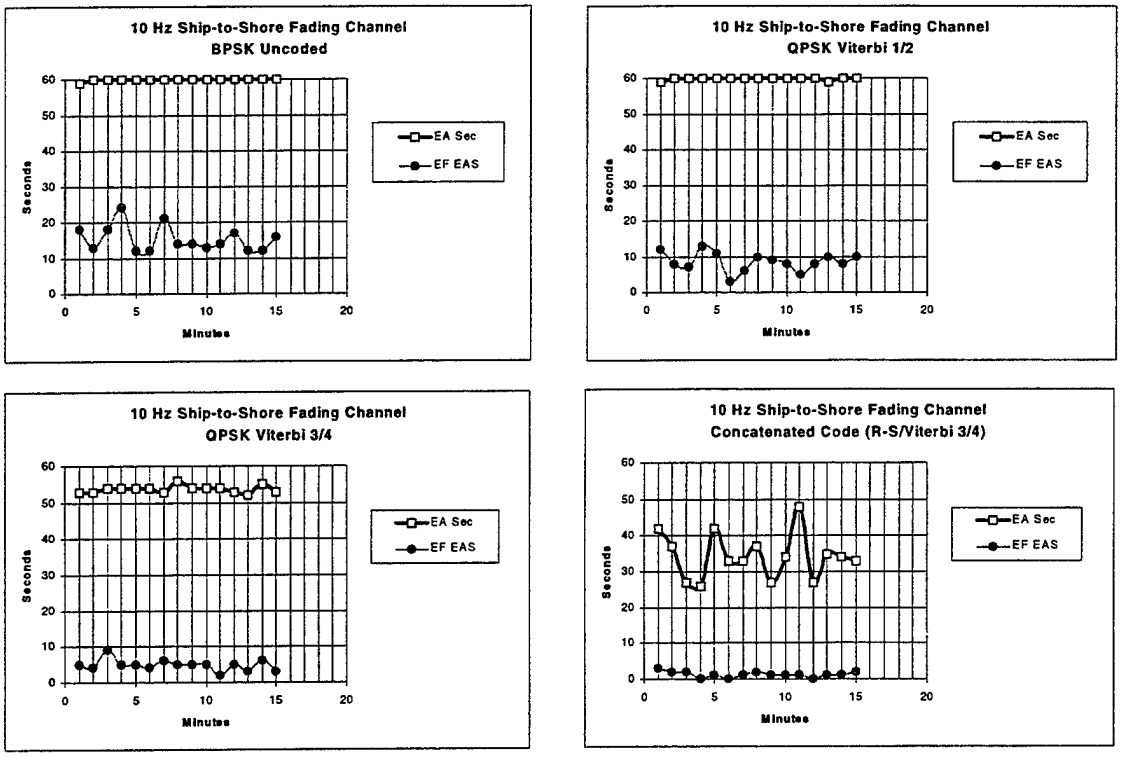

Figure 17. Standard ship-to-shore channel results (fade rate = 10 Hz).

2.4.3 "Ship-to-Air" Model

The last channels to be modeled were a slow and a standard UHF LOS ship-to-air fading channel.

2.4.3.1 Slow Ship-to-Air Model. The slow channel is modeled as:

Path #1: GSM Rician, $F_d = 1$ Hz

Path #2: Rayleigh, $T_{1\text{-}2} = 0.9$ µsec, $F_d = 1$ Hz, $L_{1\text{-}2} = -3$ dB

Path #3: Rayleigh, $T_{1\text{-}3} = 5.1$ µsec, $F_d = 1$ Hz, $L_{1\text{-}3} = -9$ dB

This model has three propagation paths with a relatively long differential delay time (5.1 usec corresponds to a differential propagation distance of about 1530 m [0.8 nmi]). This channel also has some minor frequency selectivity to it.

Figure 18 shows the slow ship-to-air channel results for BPSK Uncoded, QPSK Viterbi ½, QPSK Viterbi ¾, and QPSK R-S/Viterbi ¾. BPSK Uncoded performed worse (average EF EAS of 38 seconds) than either QPSK Viterbi ½ (average EF EAS of 45 seconds), or than QPSK Viterbi ¾ (average EF EAS of 50 seconds).

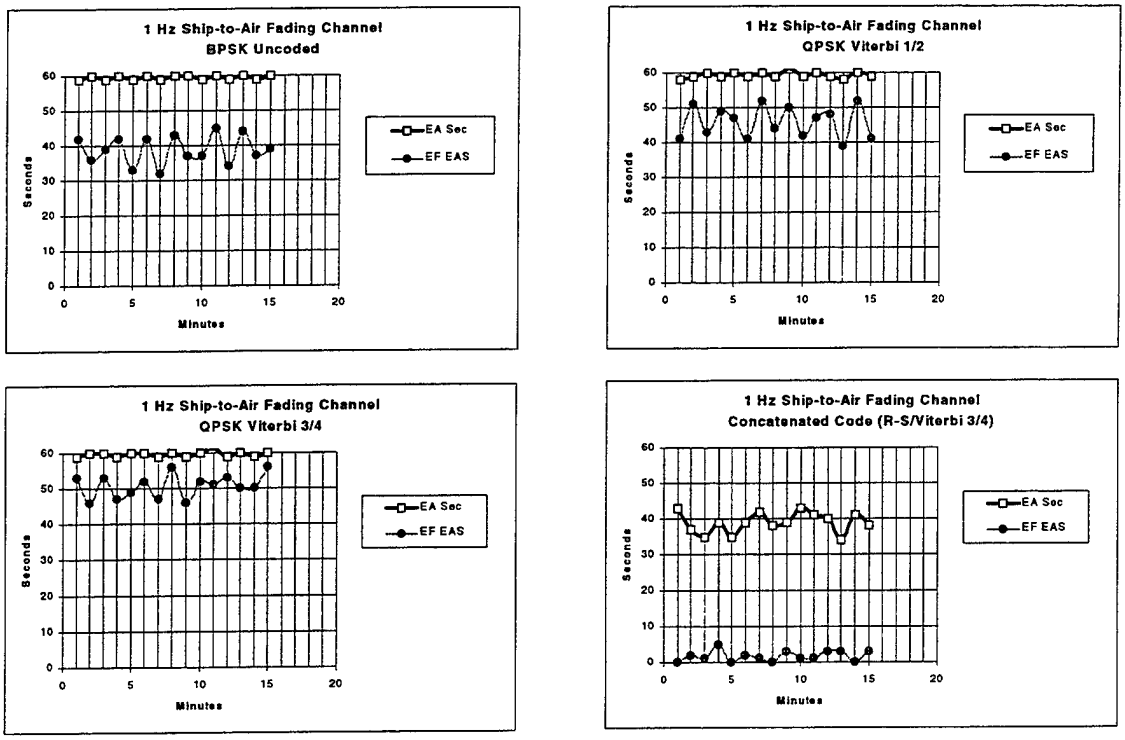

Figure 18. Slow ship-to-air channel results (fade rate = 1 Hz).

2.4.3.2 Standard Ship-to-Air Model. The standard UHF LOS ship-to-air fading channel is modeled as:

Path #1: GSM Rician, $F_d = 25$ Hz

Path #2: Rayleigh, $T_{1\text{-}2} = 0.9$ µsec, $F_d = 25$ Hz, $L_{1\text{-}2} = -3$ dB

Path #3: Rayleigh, $T_{1\text{-}3} = 5.1$ µsec, $F_d = 25$ Hz, $L_{1\text{-}3} = -9$ dB

Figure 19 shows the standard ship-to-air channel results for BPSK Uncoded, QPSK Viterbi ½, QPSK Viterbi ¾, and QPSK R-S/Viterbi ¾. This channel is clearly too dynamic for this system as all modulation schemes resulted in practically no EF EAS. Interestingly, BPSK Uncoded and QPSK Viterbi ½ still remained synchronized much of the time.

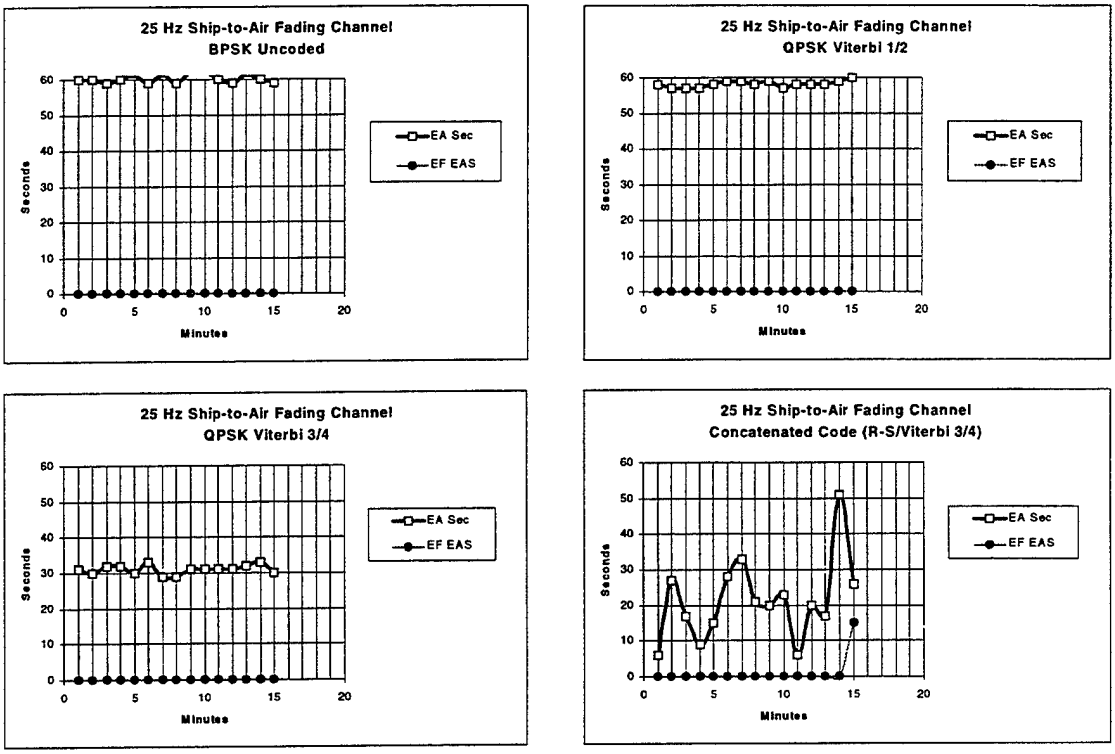

Figure 19. Standard ship-to-air channel results (fade rate = 25 Hz).

3. SAN CLEMENTE ISLAND OVER-THE-AIR TESTS

The objective of the operational tests between SSC San Diego and SCI were to explore the properties and quality of the HF surface-wave channel and compare it to the laboratory results. It was necessary to understand how the communication link reacts to different operating parameters, including modulation, coding, data rate, frequency, weather, and time of day to create a future system that is dependable and reliable.

3.1 EXPERIMENT DESCRIPTION AND SYSTEM SETUP

This section describes the results of the over-the-air operational tests conducted between Wilson Cove, San Clemente Island and Building 40, SSC San Diego, in September 1997. Figure 20 shows the system block diagram used to successfully demonstrate an Internet Protocol (IP) connection showing full-duplex applications. The equipment setup is the same as for the laboratory setup except for the addition of a computer and router on each side to test various TCP/IP applications. The SSC San Diego transmit side used an omnidirectional HF vertical antenna for transmit and a 25-ft whip for receive, both located on the roof of Building 40, SSC San Diego. The SCI transmit side used a 35-ft whip antenna for transmit and a 25-ft whip antenna for receive.

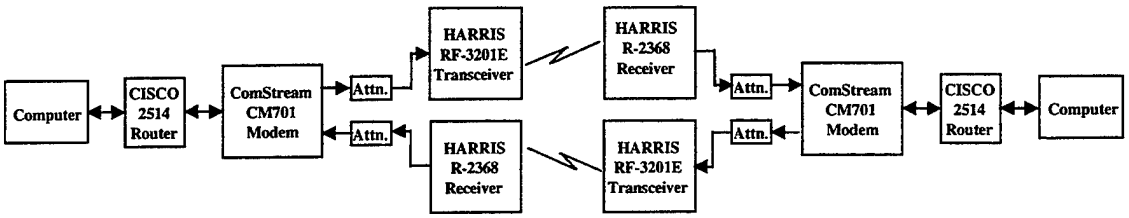

Figure 20. Equipment setup for over-the-air test to demonstrate applications.

After the application tests, the remainder of the experiments was devoted to channel-quality tests using the TTC Fireberd 6000A bit-error tester to generate data and to detect and report channel-quality results. A series of tests were performed at different times of day/night and at different HF frequencies to help determine the operational procedures that result in the best link performance. This was done at the six pre-assigned frequencies while changing data rates to explore the channel properties and how they varied. Table 3 lists the six pre-assigned frequencies.

Table 3. Pre-assigned frequencies between SSC San Diego and SCI.

Frequency Range	SCI TX Frequency (MHz)	SSC San Diego TX Frequency (MHz)
Low	6.92	4.555
Mid	10.47	11.648
High	25.46	24.42

3.2 EXPECTED PROPAGATION, FADING, AND NOISE CONDITIONS

Table 4 lists the expected propagation loss over seawater obtained from the graph in appendix A. The HF surface-wave channel over seawater was studied and described in the Advanced Research Project Agengy (ARPA) "Teal Wing" program in the 1970s. The study concluded that the HF surface-wave channel has a channel coherent bandwidth greater than the 3 to 6 kHz bandwidth normally used in the Navy. The HF surface-wave path loss is influenced by three factors, including distance, frequency, and surface quality (sea-state for over-the-water paths) (Sailors, 1997). The losses over land depend on ground conductivity and are generally much greater than the losses over seawater. Multipath propagation is not anticipated to be significant, assuming skywave propagation is avoided. Successful operation of higher data-rate HF surface-wave systems depend on achieving higher receiver signal-to-noise ratios (SNRs) suitable for the modulation scheme and the channel.

Table 4. Expected propagation loss over 65-nmi seawater path.

Frequency (MHz)	Distance over Seawater (nmi)	Propagation Loss (dB)
2	65	112
5	65	123
10	65	129
15	65	141
20	65	148
30	65	165

3.3 TEST RESULTS

The first part of the experiment successfully showed a full-duplex link over the 65-nmi seawater path between San Clemente Island and SSC San Diego. The result was a successful TCP/IP connection that demonstrated applications including whiteboarding, file transfer, application sharing, text exchange and TCP/IP voice.

The remainder of experiment time was spent observing the channel and documenting the communication link quality. The equipment setup used was exactly the same as for the laboratory tests using two sets to enable full-duplex tests. The full-duplex HF communication link worked quite well with its quality primarily depending on the surrounding background noise, interference levels, and frequency. The SSC San Diego to SCI path needed more power to link than the SCI to SSC San Diego path because of the higher background and interference noise at the SCI site.

As was done in the laboratory tests, many tests of varying parameters were conducted using the Fireberd 6000A to collect histogram data of EAS and EF EAS. These data were collected at various times of the day and night to characterize channel performance. The system worked well for the low and middle frequencies but never provided reliable communications for the high frequencies.

3.3.1 Graphed Channel Results

Observing and plotting results from the spectrum analyzer to monitor events was an important tool for gaining a better understanding of the HF surface wave channel. Many plots were taken on the SCI receive side during the day and night for the three pre-assigned SCI receive frequencies. The

graphs are located in Appendix A. Figures A-1 through A-3 show examples of a typical night background noise floor centered at each of the three SCI receive frequencies respectively. Figures A-4 through A-6 show examples of a typical day background noise floor centered at each of the three SCI receive frequencies respectively. Figures A-7 through A-9 show the entire HF spectrum covering 2 to 30 MHz for three different days and include the SCI transmit and receive signals. These clearly show the change in background interference and noise spectrum from day to day. Figures A-10 and A-11 cover 2 to 7 MHz on two different days showing this variable background spectrum in more detail. Figure A-12 shows the night version of figure A-10 and is similar except for the increased number of narrowband interferers from 4.5 to 6.5 MHz.

Many plots were taken targeting 4.555 MHz because it was the best link. Figure A-13 shows two plots during the day separated by 3 hours to show the difference in the background noise. It reveals the same receive signal with the background noise shifted. Figure A-14 shows the same picture but in the evening and shows similar results. Figure A-15 shows a plot from a different and noisier day when the system could not link because of the high background noise. The next four graphs are still centered at 4.555 MHz but vary in physical parameters including location and power. Figure A-16 shows two plots that illustrate the influence of moving the receive antenna. It shows the resulting background noise with the receive antenna in two different locations. Figure A-17 shows the influence of transmitting while receiving. It shows three plots of the receive signal: one while not transmitting, another while transmitting a 10.47-MHz signal and, lastly while transmitting a 6.920-MHz signal. This would address self-interference problems, which, as expected, are worse at 6.920 MHz than at 10.470 MHz. Figure A-18 shows the benefits of using a better receive antenna. It shows two plots with one using the receive antenna to receive and the other using the transmit antenna to receive. As expected, the transmit antenna showed better performance because it was longer, used a coupler, and had ground radials. The last figure in this group is figure A-19, which shows the receive signal when SSC San Diego increased their transmit power to 250 watts.

The next group of plots is centered at 11.648 MHz. Figure A-20 shows an example of a typical receive signal that was buried in the surrounding noise yet remained linked with an E_b/N_o of 3.5 dB. Figure A-21 shows the same picture but at night with a large interferer in the band that prevented the system from linking. Figure A-22 shows the same receive signal but during a better link the next morning.

Typically, the link functioned well at the low frequencies, good to marginal at the middle frequencies, and never at the high frequency. After a link was established, it continued strong if the noise floor continued low without any large interferers in the band.

3.3.2 SSC San Diego to SCI Results

Figure 21 shows four 60-minute EAS and EF EAS graphs for the channel from SSC San Diego to SCI. The same four modulation and coding types are used that were used for the laboratory tests. SCI was receiving SSC San Diego's signal with an average E_b/N_o of 10 dB during these tests. The communication link was most reliable with QPSK Viterbi ½, which had an average EF EAS of over 59 seconds each minute. QPSK Viterbi ¾ also performed well with an average of 57.5 seconds each minute. The BPSK Uncoded results did well for EAS but received no EF EAS. The concatenated coded results received no EAS and EF EAS because the system could not maintain the synchronization needed for the additional block coding.

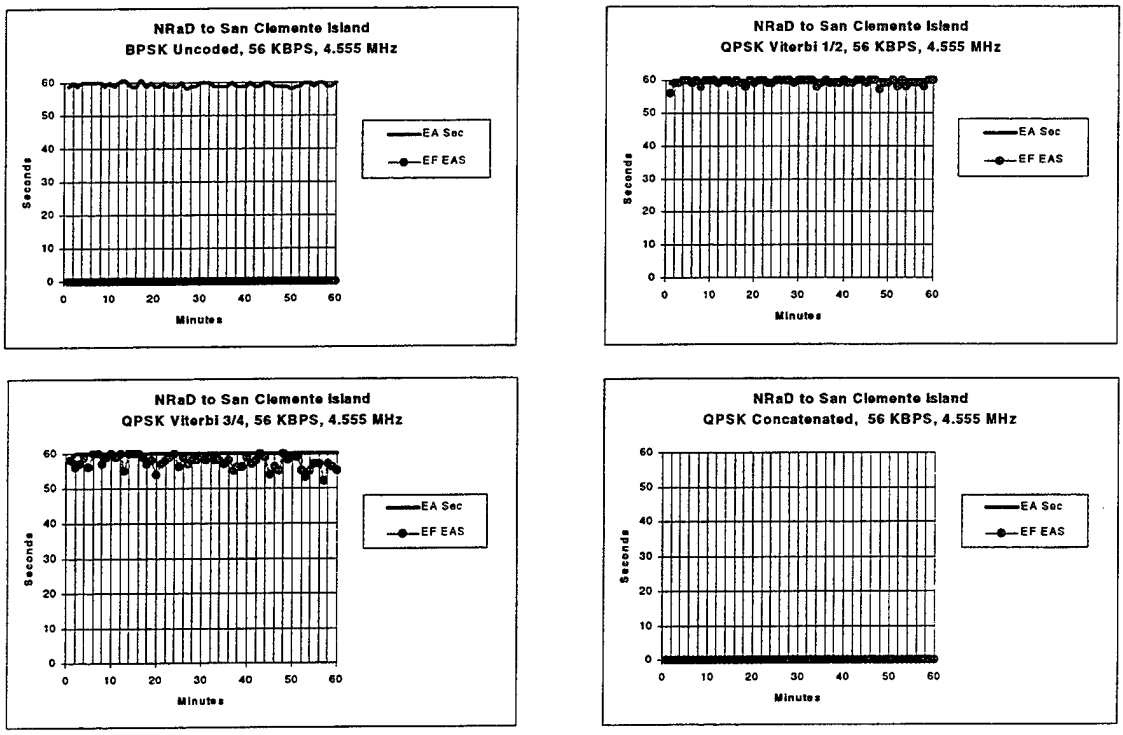

Figure 21. SSC San Diego to San Clemente Island channel results.

3.3.3 SCI to SSC San Diego Results

Figure 22 shows four 60-minute EAS and EF EAS graphs for the channel from SCI to SSC San Diego. The same four modulation and coding types are used that were used for the laboratory tests. SSC San Diego was receiving SCI's signal with an average E_b/N_o of 5 dB during these tests. Again, QPSK Viterbi ½ provided the most reliable communication link with an average EF EAS of over 56 seconds each minute, while QPSK Viterbi ¾ provided an average EF EAS of 43 seconds each minute. The BPSK Uncoded results did well again for EAS but received no EF EAS. The concatenated coded results again received no EAS and EF EAS because the system could not maintain the synchronization needed for the additional block coding.

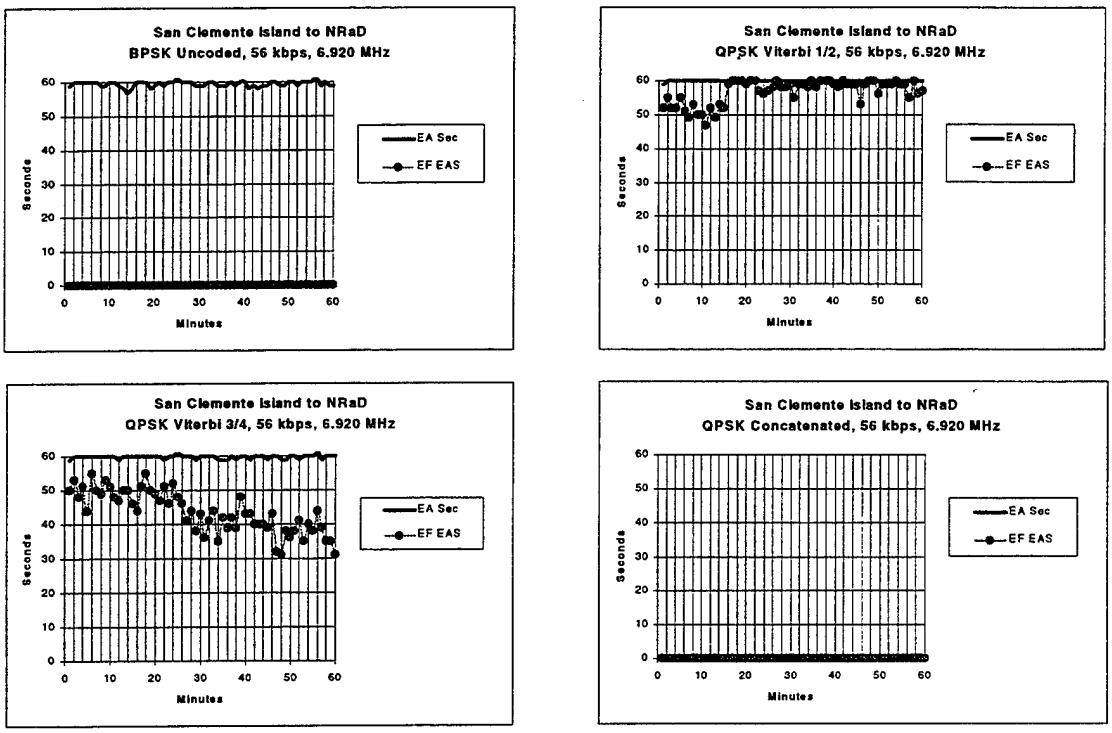

Figure 22. SCI to SSC San Diego channel results.

Figures 23 through 25 each show a 60-minute EF EAS graph for the channel from SCI to SSC San Diego for QPSK Viterbi ½ that varied either the data rate or frequency.

Figure 23 shows two plots at 6.92 MHz that compare results at 25 and 64 kbps. The 25 kbps results perform better with an average EF EAS equal to 57 seconds each minute, while the 64 kbps results have an average EF EAS equal to 48 seconds each minute. It was expected that the higher data rate of 64 kbps (64 ksps) would perform worse because (1) it requires 4 dB more SNR due to the increased data rate, and (2) it was band-limited by the R-2368/URR Receiver (additional ISI loss).

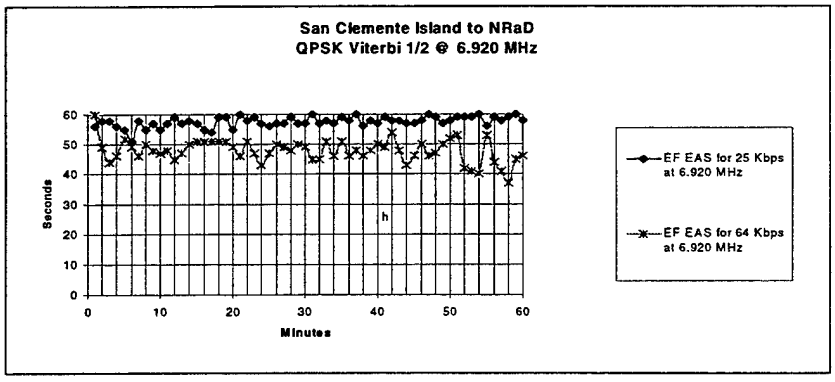

Figure 23. SCI to SSC San Diego test at 6.92 MHz.

Figure 24 shows two plots at 13.2 MHz that compare results at 25 and 56 kbps. The 25 kbps results perform better with an average EF EAS equal to 36 seconds each minute, while the 56 kbps results have an average EF EAS equal to 27 seconds each minute.

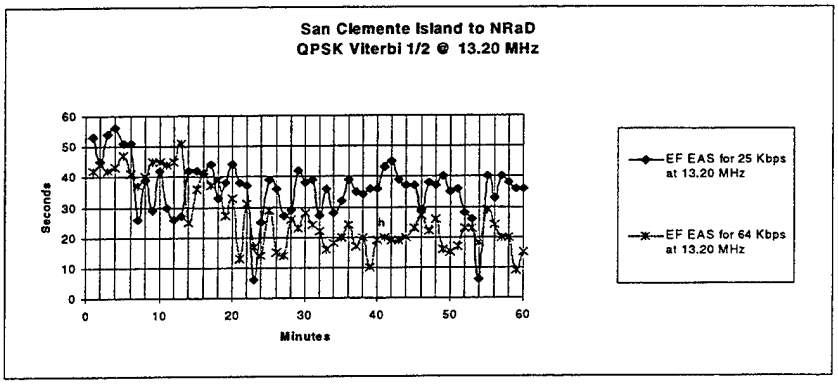

Figure 24. SCI to SSC San Diego test at 13.2 MHz.

Figure 25 shows two plots at 25 kbps, each from figure 23 and 24 above, that compare results at 6.92 MHz and 13.2 MHz. The 6.92 MHz EF EAS results perform better with an average of 30 seconds each minute higher than the 13.2 MHz results, indicating that the HF surface wave is more prominent and stable at the lower HF frequencies.

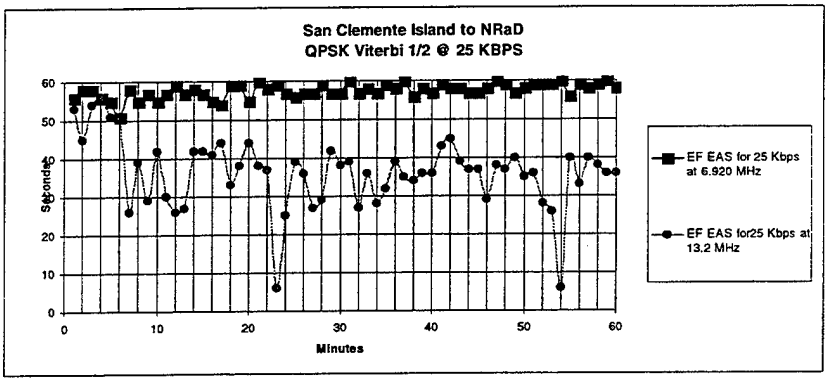

Figure 25. SCI to SSC San Diego test at 25 kbps.

3.3.4 Overnight Tests

The following overnight full-duplex tests are conducted at the low frequencies for 24 hours starting at 2:30 pm. Figure 26 shows the two graphs. The top graph shows the EF EAS results transmitted from SSC San Diego to SCI at 64 kbps QPSK Viterbi ½ at 4.555 MHz, while the lower graph shows the EF EAS results transmitted from SCI to SSC San Diego at 56 kbps QPSK Viterbi ½ at 6.92 MHz.

Skywave Propagation theory predicts that lower frequencies will propagate better at night, while higher frequencies will propagate better during the day. This could have an adverse effect on the HF surface wave communication link due to an increase in the number of interfering signals at night. The SNR decreases because the noise level increases. It appears that this may have happened in the bottom graph of figure 26 because the EF EAS decrease around 5:30 p.m. and begin to improve about 5:15 am. This is not the case for the top graph because EF EAS increased around 5 pm and remain at an average of 30 EF EAS each minute until 12 p.m. the following day. It is difficult to evaluate the overnight tests because background noise, interferers, and diurnal propagation effects influence the signal quality.

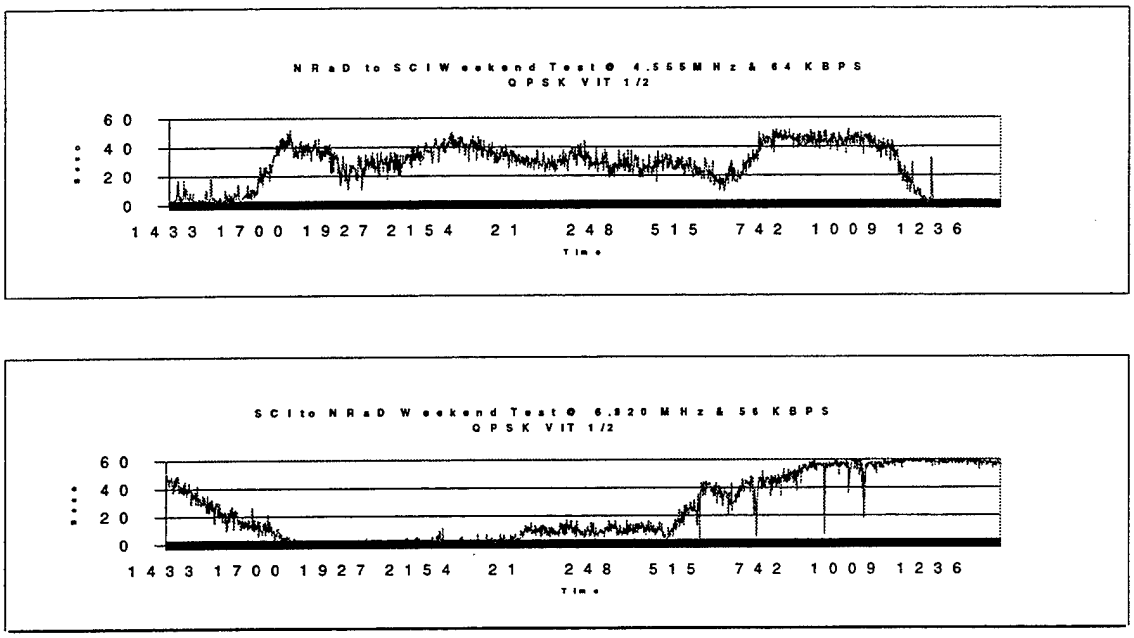

Figure 26. Overnight test between SSC San Diego and SCI.

4. CONCLUSIONS

This report describes many MDR HF BLOS communication experiments and tests to prove the feasibility of using higher data rate over HF in the U.S. Navy. Modern communication demands create a tremendous need for additional bandwidth that this technology can help support. In coordination with current high-data-rate UHF LOS link projects, MDR HF can provide the BLOS RF links to support implementation of higher capacity communication links and networking technologies. This will dramatically improve transport of data, greatly reduce dependence on "stove-pipe" communication systems, and improve carrier battle group (CVBG) and amphibious task group (ATG) operations efficiency.

The system is based on commercial products as well as existing radio equipment with simple modifications. The experiments included laboratory baseline characterization, static multipath and dynamic multipath performance tests and an over-the-air operational test performed over the 65 nmi seawater path between SCI and SSC San Diego. Many variations of different operating parameters including modulation, coding and frequency selection were tested over the MDR HF BLOS link within a 50-kHz bandwidth to increase its bandwidth efficiency.

It was confirmed that the HF surface-wave channel over seawater is basically a benign channel that is primarily degraded by distance, frequency, and interferers. As expected for surface wave, the results of the laboratory and operational tests show that lower frequencies propagate better than higher frequencies. Many modulation and coding combinations were tested and QPSK Viterbi ¾ and ½ clearly outperformed the other combinations in the laboratory as well as in the operational tests. The QPSK Viterbi ¾ results in the laboratory tests seemed similar to the QPSK Viterbi ½ results against multipath interference but performed better because of its reduced transmitted bandwidth. However, QPSK Viterbi ½ outperformed QPSK Viterbi ¾ during the over-the-air tests between SCI and SSC San Diego by performing better and more consistent.

The achieved goal of the operational tests between SCI and SSC San Diego was to measure how the communication link reacts to different operating parameters and compare it to the results obtained in the laboratory. The next logical and needed step is a true operational experiment between two deployed Navy ships during a Navy Exercise. This will be accomplished between the USS Coronado and the USS Cleveland during RIMPAC-98 in July and August 1998 . The MDR HF equipment was installed and will be demonstrated and tested between these two ships to further analyze and improve this system. The continued goal is to prove the feasibility of the successful use of higher data rate HF links within the U.S. Navy, with proper modulation, coding and frequencies, for improved intership BLOS communications.

5. REFERENCES

Danielson, T. 1997. "Efficient, High Capacity Extended Range Links for the Expeditionary Warfare Environment," ONR FY 98 Proposal (May). Office of Naval Research, Arlington, VA.

North, R. C. et. al. 1995. "Use of the AN/WSC-3 External Modem Interface for High-Data-Rate UHF Digital Communication: Experimental Results," Technical Report 1701(May). Space and Naval Warfare Systems Center, San Diego, CA.

Sailors, D. 1997. "Excess System Power Available for Short-Range, High-Frequency Communication Systems," Technical Document 2978 (Aug). Space and Naval Warfare Systems Center, San Diego, CA.

Sklar, B. 1988. *Digital Communications Fundamentals and Applications*, Prentice Hall, Englewood Cliffs, NJ.

Yacoub, M. D. 1993. *Foundations of Mobile Radio Engineering*, CRC Press, Boca Raton, FL.

APPENDIX A

GRAPHED CHANNEL RESULTS

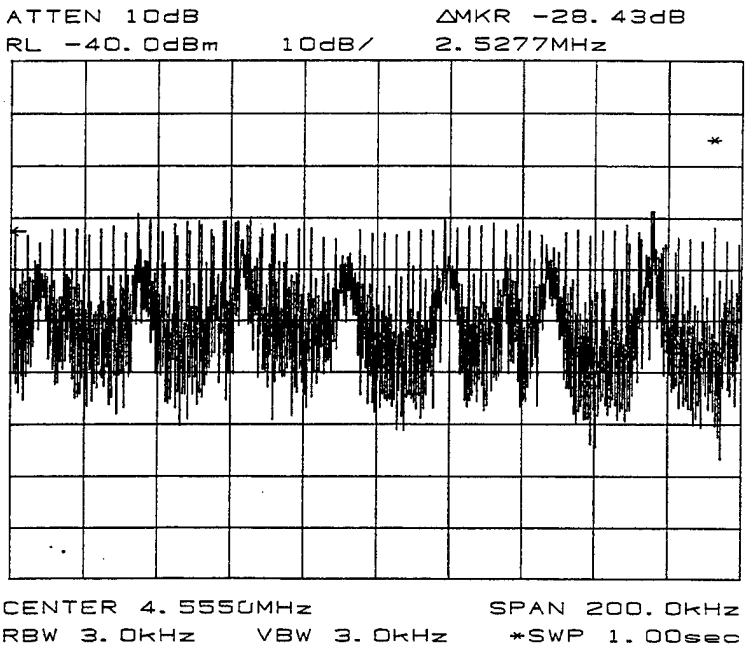

Figure A-1. Background noise at night centered at 11.648 MHz.

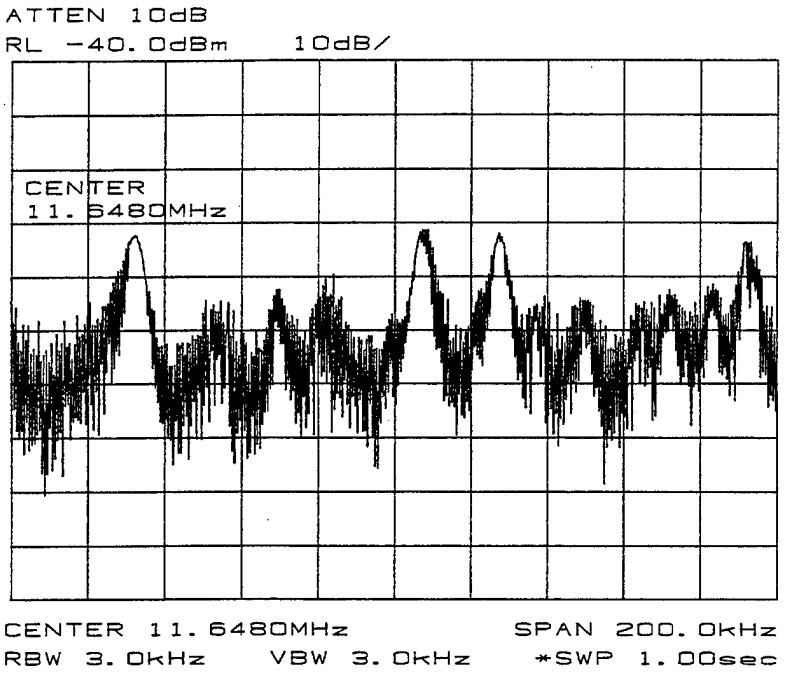

Figure A-2. Background noise at night centered at 4.555 MHz.

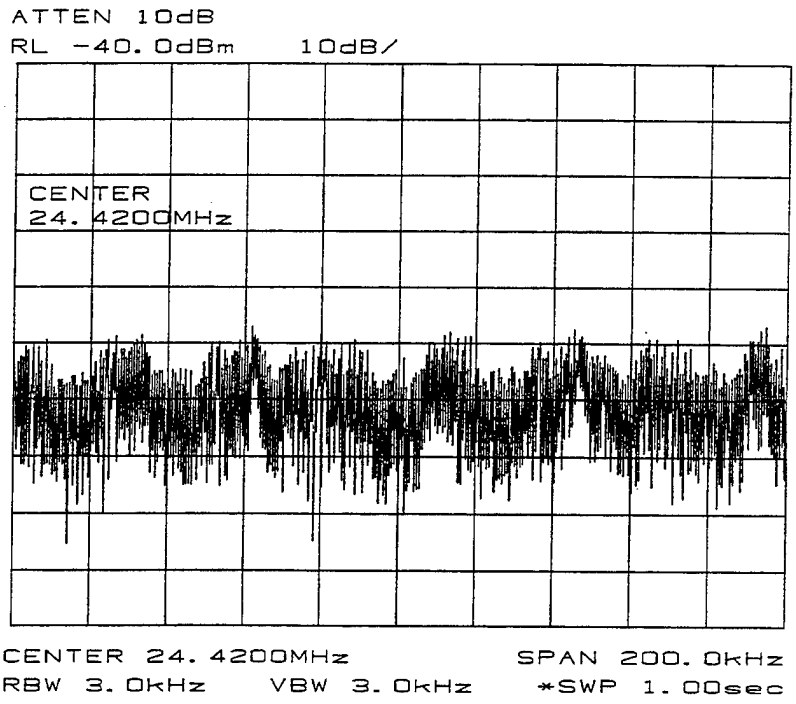

Figure A-3. Background noise at night centered at 24.42 MHz.

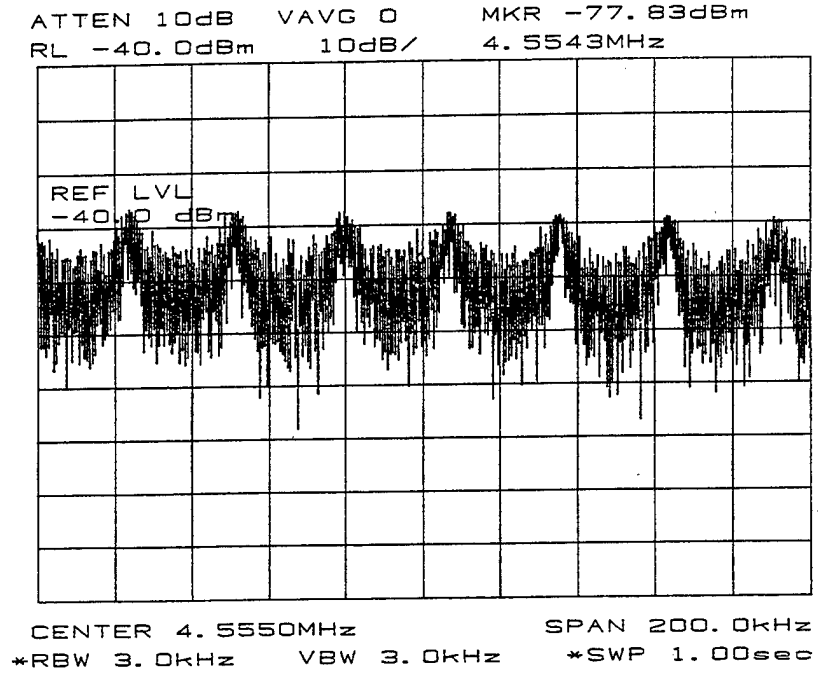

Figure A-4. Background noise during the day centered at 4.555 MHz.

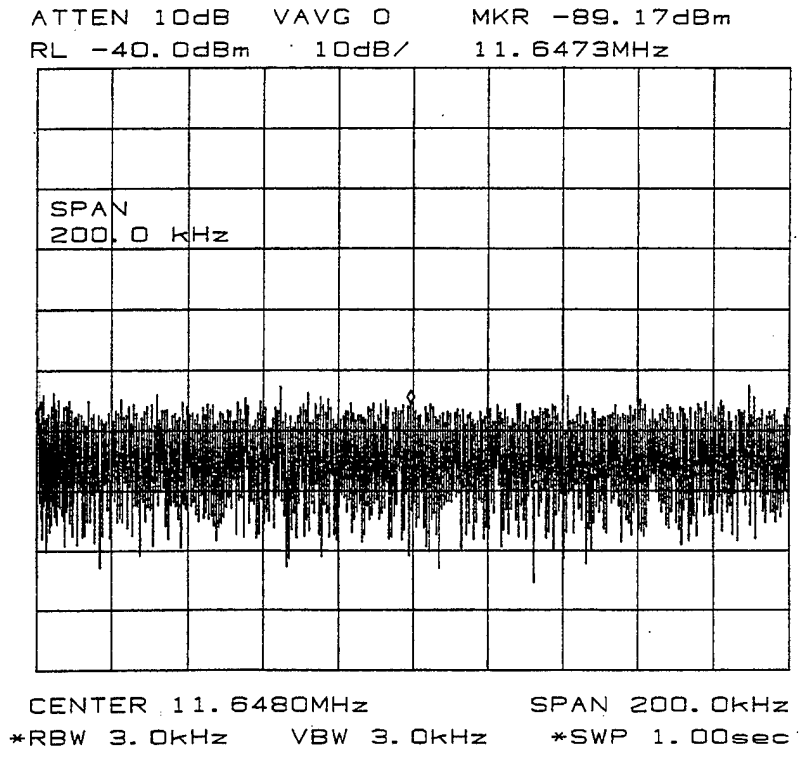

Figure A-5. Background noise during the day centered at 11.648 MHz.

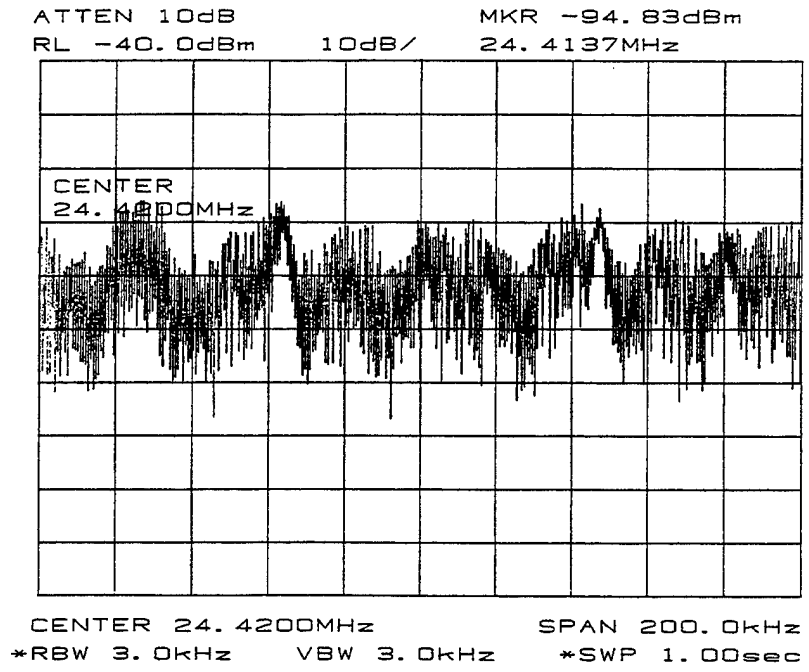

Figure A-6. Background noise during the day centered at 24.42 MHz.

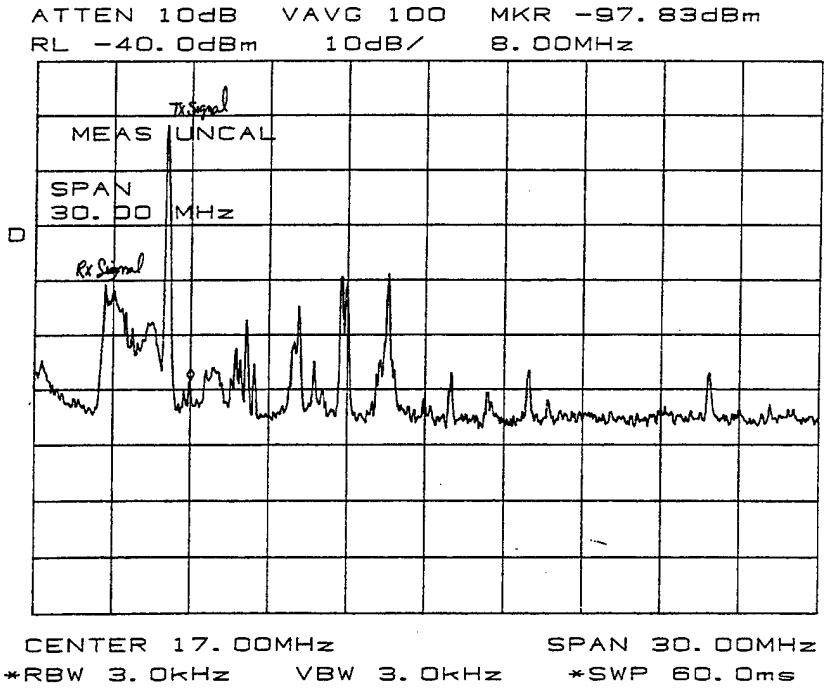

Figure A-7. Entire HF day spectrum including SCI TX and RX signals (9 September 1997).

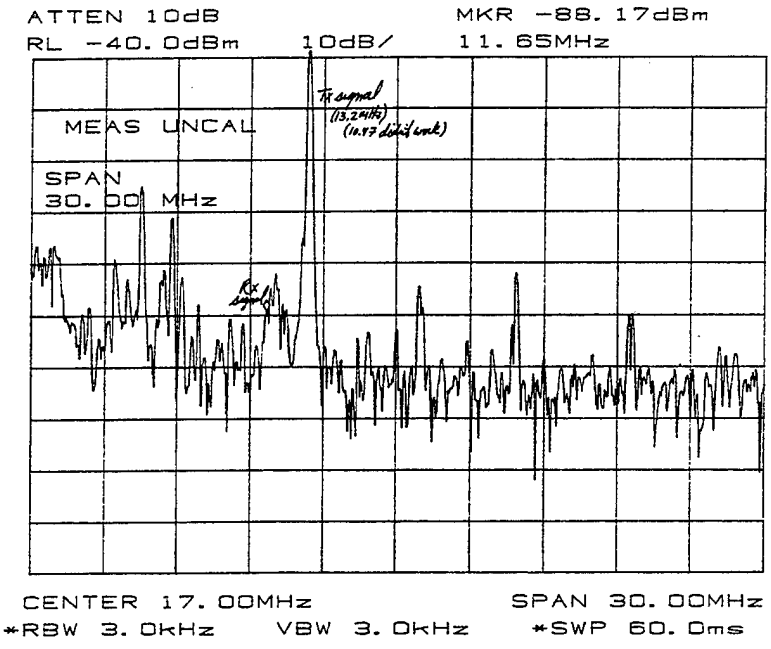

Figure A-8. Entire HF day spectrum including SCI TX and RX signals (10 September 1997).

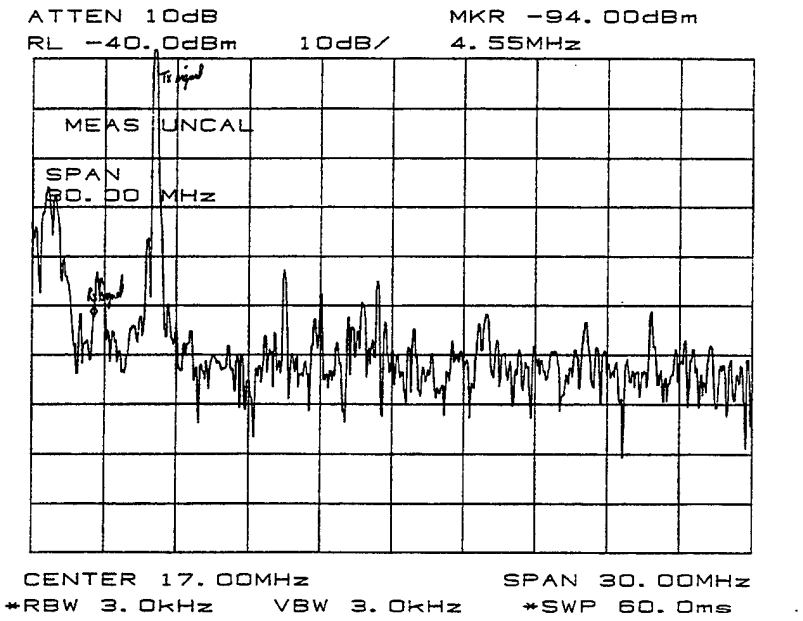

Figure A-9. Entire HF day spectrum including SCI TX and RX signals (11 September 1997).

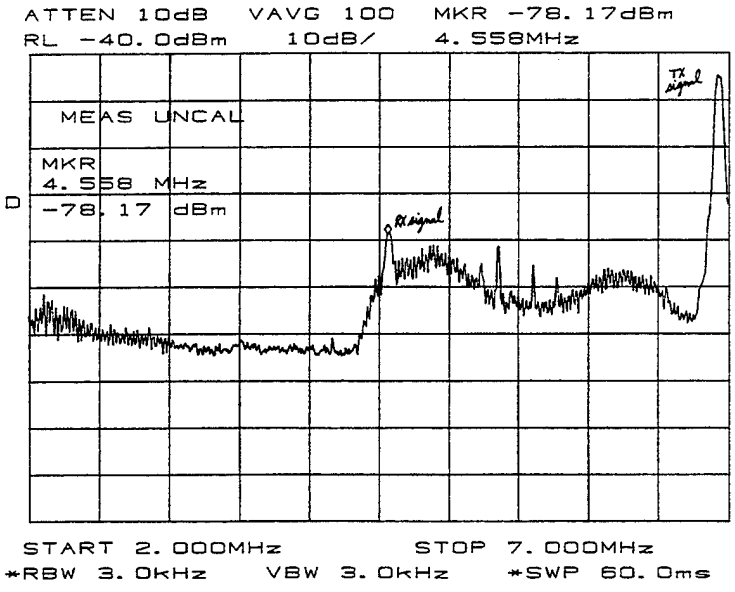

Figure A-10. 2 to 7 MHz HF day spectrum including SCI TX and RX signals (9 September 1997).

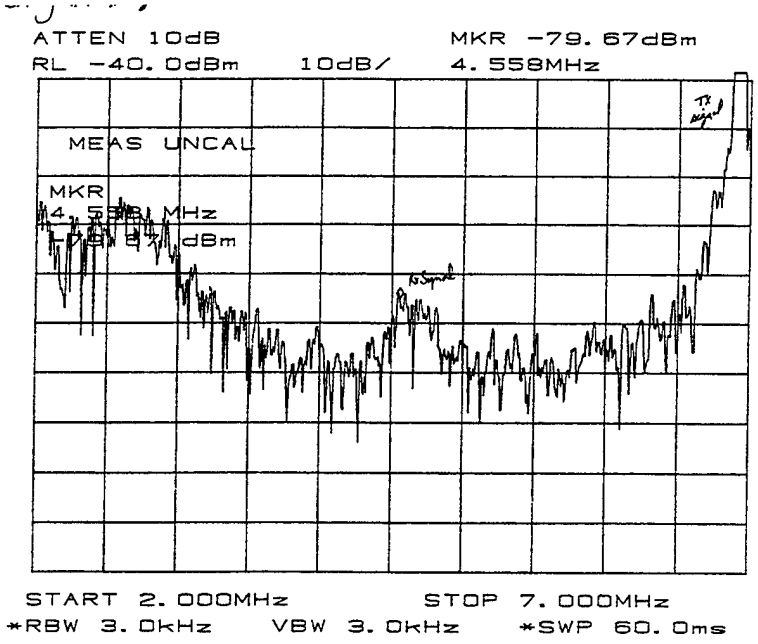

Figure A-11. 2 to 7 MHz HF day spectrum including SCI TX and RX signals (10 September 1997).

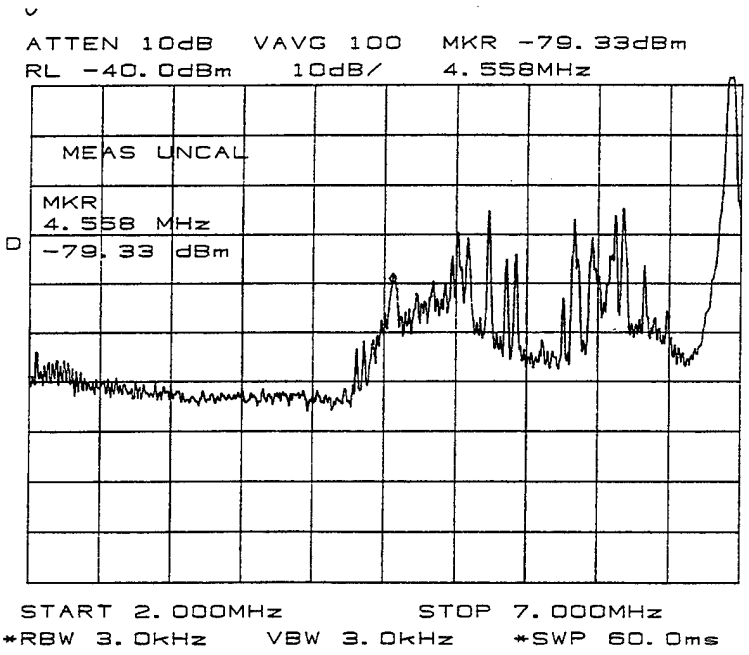

Figure A-12. 2 to 7 MHz HF night spectrum including SCI TX and RX signals (night version of figure A-10)

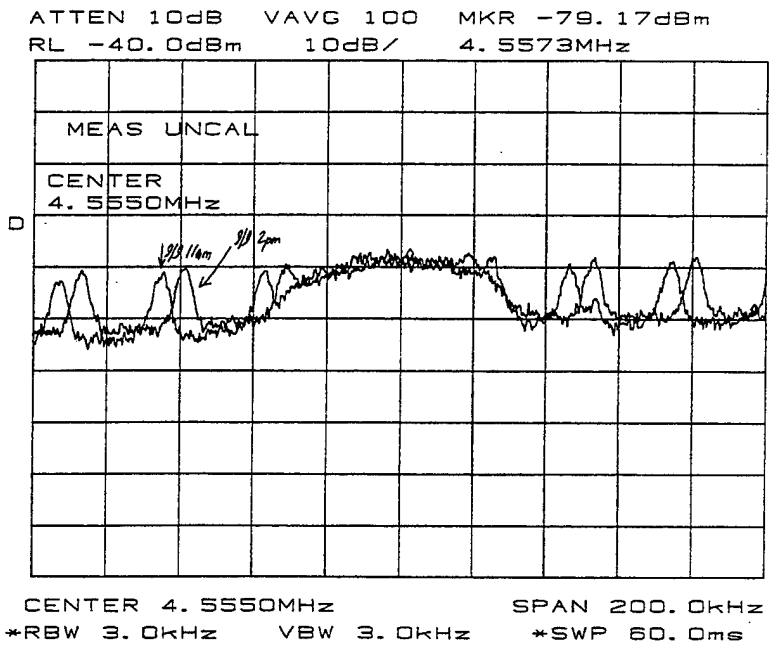

Figure A-13. Two plots of the wideband RX signal at 4.555 MHz separated by 3 hours during the day (10 September 1997).

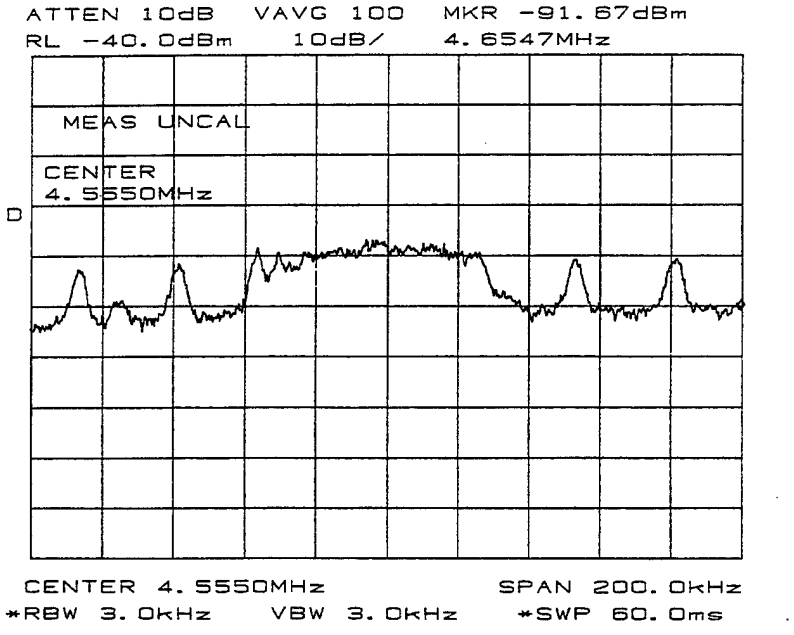

Figure A-14. Wideband RX signal at 4.555 MHz in the evening of figure A-13.

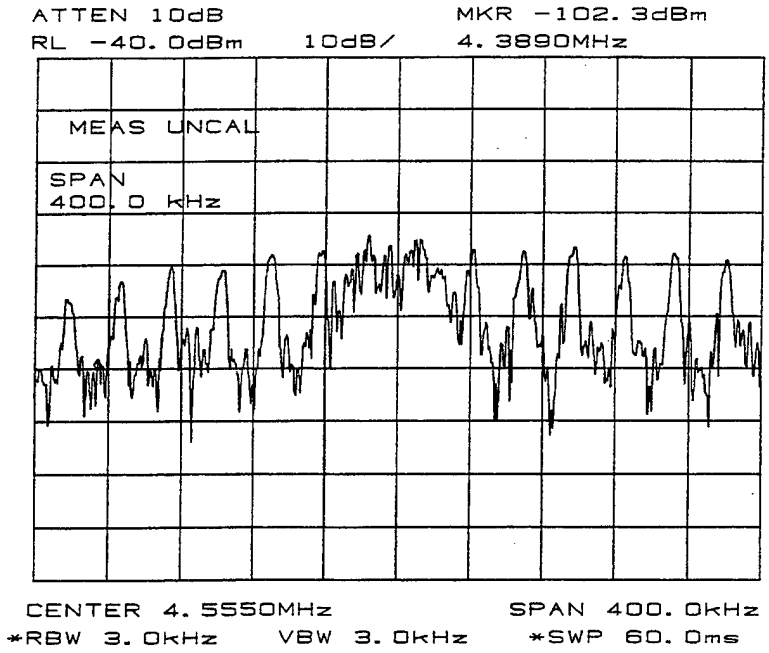

Figure A-15. Wideband RX signal at 4.555 MHz during a noisy day so the system could not link.

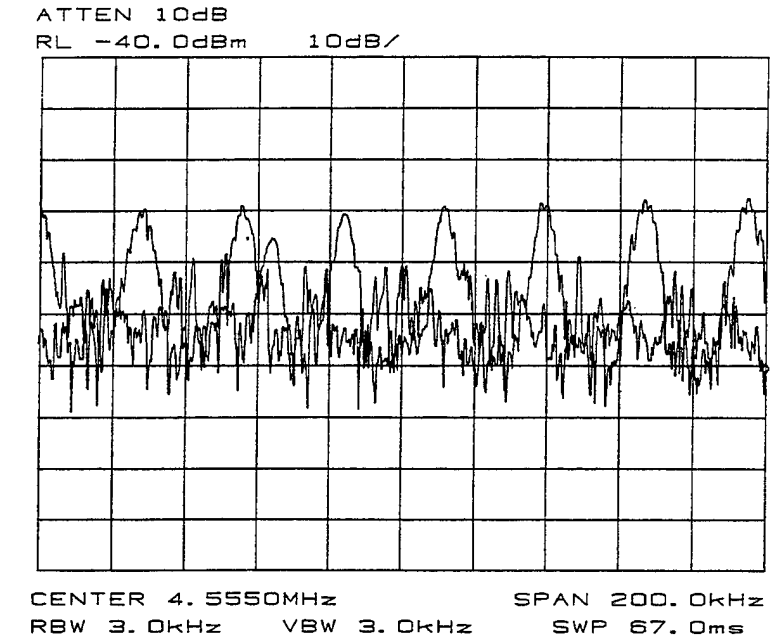

Figure A-16. Two plots of the background noise centered at 4.555 MHz with the RX antenna in different locations.

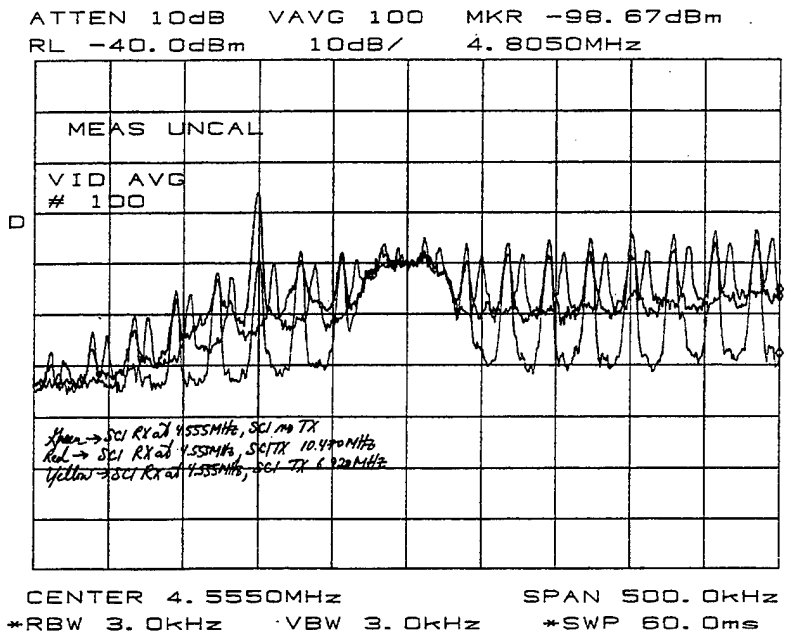

Figure A-17. Three plots of the wideband RX signal at 4.555 MHz showing the influence of transmitting while receiving.

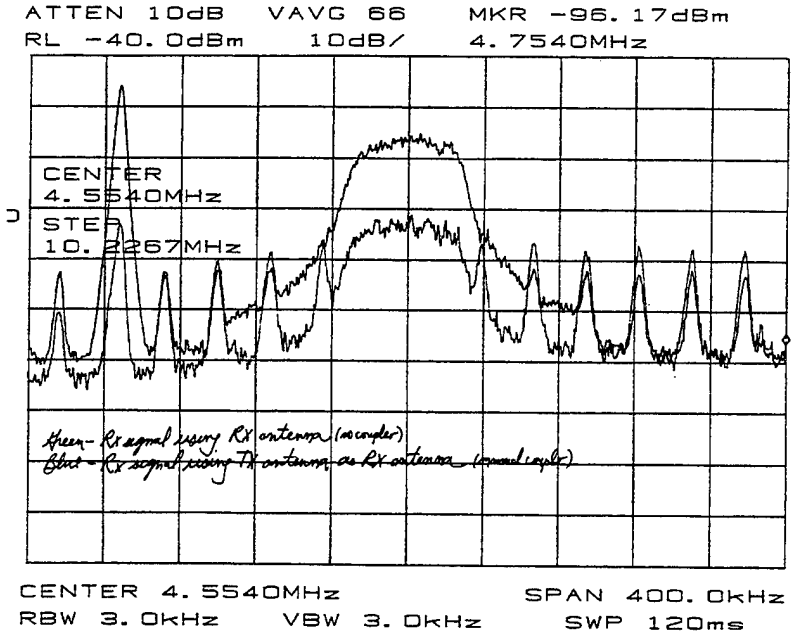

Figure A-18. Two plots of the wideband RX signal at 4.554 MHz showing the benefit of a better RX antenna.

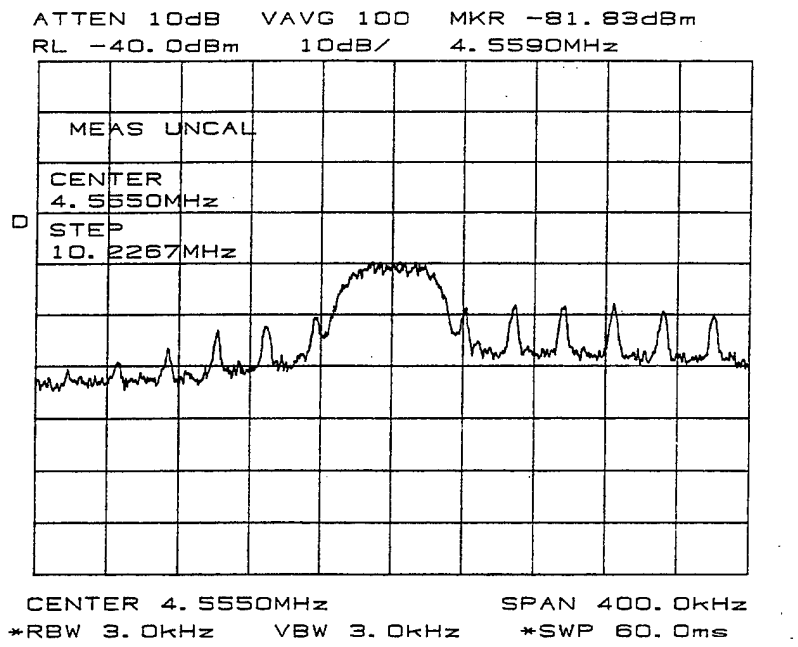

Figure A-19. Wideband RX signal at 4.555 MHz after SSC San Diego increased transmit to 250 watts.

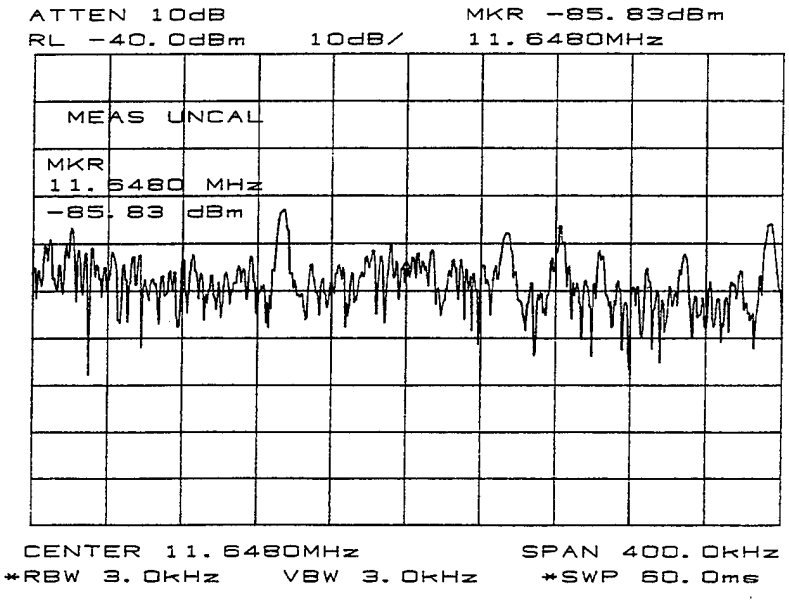

Figure A-20. Wideband RX day signal at 11.648 MHz almost buried in noise yet remains linked.

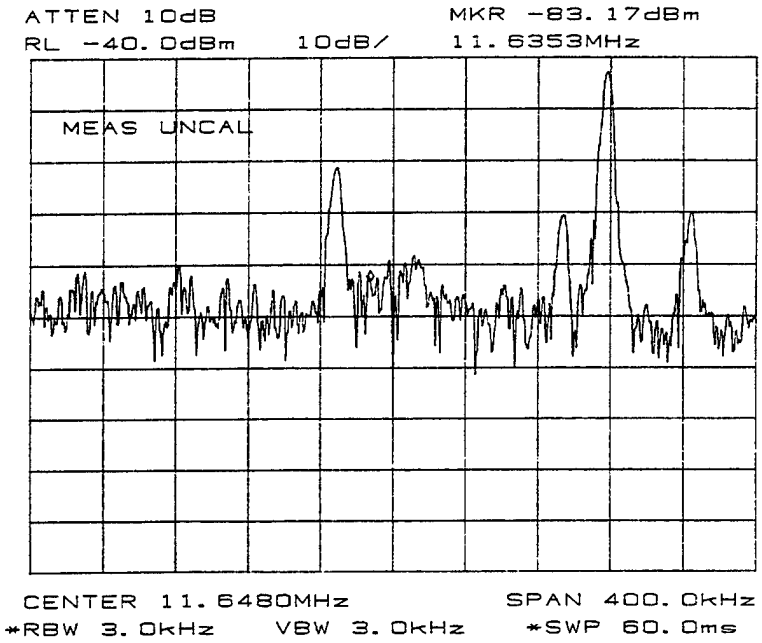

Figure A-21. Wideband RX night signal at 11.648 MHz with in-band interferer preventing link.

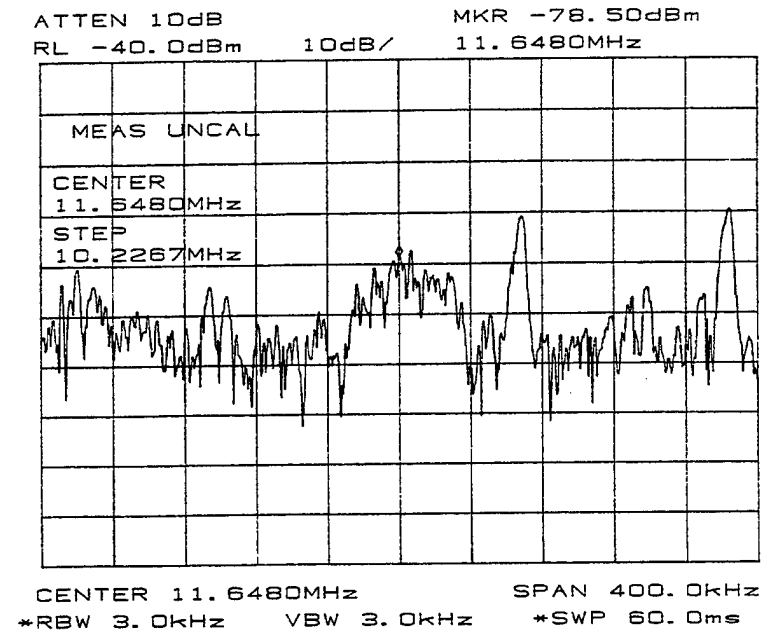

Figure A-22. Well-linked wideband RX day signal at 11.648 MHz.

REPORT DOCUMENTATION PAGE

Form Approved
OMB No. 0704-0188

1. AGENCY USE ONLY *(Leave blank)*	2. REPORT DATE	3. REPORT TYPE AND DATES COVERED
	March 1998	Final: March – September 1997

4. TITLE AND SUBTITLE

MEDIUM-DATA-RATE HF EXPERIMENTAL TEST RESULTS

Using Modified Harris RF–3201E Transceiver and R–2368/URR Receiver

5. FUNDING NUMBERS

PE: 0602232N
AN: DN307634
WU: CJ03

6. AUTHOR(S)

L. H. Pinck, T. A. Danielson, R. North

7. PERFORMING ORGANIZATION NAME(S) AND ADDRESS(ES)

Space and Naval Warfare Systems Center, San Diego
San Diego, CA 92152–5001

8. PERFORMING ORGANIZATION REPORT NUMBER

TR 1766

9. SPONSORING/MONITORING AGENCY NAME(S) AND ADDRESS(ES)

Office of Naval Research
800 North Quincy Street
Arlington, VA 22217–5660

10. SPONSORING/MONITORING AGENCY REPORT NUMBER

11. SUPPLEMENTARY NOTES

12a. DISTRIBUTION/AVAILABILITY STATEMENT

Approved for public release; distribution is unlimited.

12b. DISTRIBUTION CODE

13. ABSTRACT *(Maximum 200 words)*

This report describes the experimental test results of a medium-data-rate (MDR), high-frequency (HF) groundwave point-to-point, full-duplex data link. This system uses relatively simple modifications of existing radio equipment and a commercial programmable satellite communications (SATCOM) modem. The goal is to develop and implement a 128-kbps Beyond-Line-Of-Sight (BLOS) HF communication link within a 50-kHz, 3-dB bandwidth frequency channel. This is one of several efforts that attempts to increase the data rates that are commonly used in the HF band within the Navy for intraship BLOS communications.

The tests performed included laboratory back-to-back and over-the-air operational tests. The laboratory portion of these tests was performed at Space and Naval Warfare (SPAWAR) Systems Center, San Diego (SSC San Diego), primarily between March and June of 1997. In September 1997, the over-the-air tests were conducted over the 65-nmi seawater path between Wilson Cove at San Clemente Island (SCI), California, and Building 40, SSC San Diego, on Point Loma, California.

14. SUBJECT TERMS

Mission Area: Command, Control and Communications
high frequency
medium data rate
beyond-line-of-sight communications link

15. NUMBER OF PAGES

56

16. PRICE CODE

17. SECURITY CLASSIFICATION OF REPORT	18. SECURITY CLASSIFICATION OF THIS PAGE	19. SECURITY CLASSIFICATION OF ABSTRACT	20. LIMITATION OF ABSTRACT
UNCLASSIFIED	UNCLASSIFIED	UNCLASSIFIED	SAME AS REPORT

21a. NAME OF RESPONSIBLE INDIVIDUAL	21b. TELEPHONE *(include Area Code)*	21c. OFFICE SYMBOL
L. H. Pinck	(619) 553–1399 e–mail: pinck@spawar.navy.mil	Code D846

INITIAL DISTRIBUTION

Code D0012	Patent Counsel	(1)
Code D0271	Archive/Stock	(6)
Code D0274	Library	(2)
Code D027	M. E. Cathcart	(1)
Code D0271	D. Richter	(1)
Code D176–3	S. Valvonis	(1)
Code D451	R. Hollandsworth	(1)
Code D604	C. Moussa	(1)
Code D7213	B. Satterlee	(1)
Code D73J	J. Audia	(1)
Code D8203	R. Merk	(1)
Code D824	H. Guyader	(1)
Code D832	G. Crane	(1)
Code D8405	G. Clapp	(1)
Code D8405	C. Fuzak	(1)
Code D841	R. Axford	(1)
Code D846	T. Danielson	(10)
Code D846	J. Ramos	(1)
Code D846	C. Liou	(10)
Code D846	H. Wiesenfarth	(1)
Code D846	P. Francis	(1)
Code D851	P. Li	(1)
Code D855	R. North	(1)
Code D856	D. Tam	(1)
Code D88	J. Richter	(1)
Code D8805	D. Gingras	(1)
Code D882	J. Ferguson	(2)
Code D882	D. B. Sailors	(15)
Code D882	R. Sprague	(1)

Defense Technical Information Center
Fort Belvoir, VA 22060–6218 (4)

SPAWARSYSCEN Liaison Office
Arlington, VA 22202–4804

Center for Naval Analyses
Alexandria, VA 22302–0268

Navy Acquisition, Research and Development
Information Center (NARDIC)
Arlington, VA 22244–5114

GIDEP Operations Center
Corona, CA 91718–8000

Lisa Pinck
Los Angeles, CA 90035

Space and Naval Warfare Systems Command
Arlington, VA 22245–5200 (2)

Space and Naval Warfare Systems Command
San Diego, CA 92110–3127 (5)

Office of Naval Research
Arlington, VA 22217–5660 (4)

Navy Research Laboratory
Washington, DC 20375–5000 (2)

USA CECOM
Ft. Monmouth, NJ 07703–5000 (3)

Naval Surface Warfare Center
Coastal Systems Station
Dahlgren Division
Panama City, FL 32407–7001 (2)

USAF RADC
Rome, NY 13441–4505 (2)

Chief of Naval Operations
Washington, DC 20350–2000 (2)

DOD Joint Spectrum Center
Annapolis, MD 21402–5064 (3)

Naval Electromagnetic Spectrum Center
Washington, DC 20394–5460